UNIVERSITY OF CALGARY

Why It Is Hard to See Schrödinger's Cat:
Micro-Macro Entanglement under Coarse-grained Measurements

by

Sadegh Raeisi

A THESIS
SUBMITTED TO THE FACULTY OF GRADUATE STUDIES
IN PARTIAL FULFILLMENT OF THE REQUIREMENTS FOR THE
DEGREE OF MASTER OF SCIENCE

DEPARTMENT OF PHYSICS AND ASTRONOMY

INSTITUTE FOR QUANTUM INFORMATION SCIENCE

CALGARY, ALBERTA
AUGUST, 2011

© Sadegh Raeisi 2011

UNIVERSITY OF CALGARY

FACULTY OF GRADUATE STUDIES

The undersigned certify that they have read, and recommend to the Faculty of Graduate Studies for acceptance, a thesis entitled "Why it is hard to see Schrödinger's cat" submitted by Sadegh Raeisi in partial fulfillment of the requirements for the degree of MASTER OF SCIENCE.

Supervisor, Dr. Christoph Simon
Department of Physics and Astronomy

Dr. Jörn Davidsen
Department of Physics and Astronomy

Dr. Reyhaneh Safavi-Naeini
Department of Computer Science

Aug 22, 2011
Date

Abstract

The border between classical physics and quantum mechanics has been puzzling physicists since the early days of quantum mechanics. There are some approaches to explain the Quantum-to-Classical transition e.g. the decoherence program. Here I stick to a recent approach which places the emphasis on the precision of measurements. I use this approach to explain why it is difficult to observe Schrödinger's cat.

To do so, I focus on a physical realization of Schrödinger's cat which was reported in [4]. In this experiment, De Martini et al. amplify one photon of a singlet state to a macroscopic beam of light. I compare this Schrödinger's cat to a system with pure classical correlation and show that if photon counting measurements on the amplified beam are coarse-grained, then the statistics of the system in De Martini's experiment can be reproduced by a classical correlation.

Acknowledgements

First and foremost I offer my sincerest gratitude to my family, who has been supporting me for all these years and helped me feel safe when life was stormy. They have been always there to listen to my problems and to help me with their advices, supports and sometimes just with their pleasant smiles.

I also would like to thank all those who helped me scientifically and professionally; my supervisor, Christoph Simon who helped me a lot with my project; Barry C. Sanders, who was my primary supervisor and helped me to find my way through my studies as a graduate student; Wolfgang Tittel, Jörn Davidsen and Nathan Weibe for useful discussions.

At last but not least, I should acknowledge all my friends and friendships, specially I should thank Saleh, who was a friend to me before he even knew me and helped me to settle down when I first got to Calgary and knew no one here. I also thank Khabat, Jalal, Rooholah, Amir, Maryam, Farid, Razieh, Zahra, Hamid, Nasrin and many others who helped me with my life in Calgary and made it comfortable and more liveable. Finally, I thank Laleh and Sima who were always there to listen to me when I was sad, upset or excited and needed a friend to tell him or her about what made me feel so.

I acknowledge AITF, NSERC and iCORE for financial support.

Dedicated to

my grandma, who thought me to love,

and to

my parents who thought me to stand up for what I want and to be patient and persistent achieving them.

Table of Contents

Approval Page ii
Abstract iii
Acknowledgements iv
Table of Contents vi
List of Tables viii
List of Figures ix
1 Introduction 1
2 Background 3
2.1 Entanglement 3
  2.1.1 Definition 3
  2.1.2 Detection of entanglement 4
2.2 Quantum cloning 8
  2.2.1 No-cloning theorem 9
  2.2.2 Approximate cloning 10
  2.2.3 Physical realization of different cloning machines 12
2.3 Micro-Macro entanglement 17
  2.3.1 Micro-Macro entanglement in optical systems 17
  2.3.2 My project 22
2.4 Classical-to-Quantum transition and coarse-grained measurements 22
  2.4.1 Coarse-graining in spin system 23
  2.4.2 Coarse-graining in De Martini's experiment 25
3 Micro-Macro Entanglement Under Equatorial Coarse-grained Measurements 26
3.1 Problem 26
3.2 Method 28
  3.2.1 Micro-Macro system with classical correlation 29
  3.2.2 Probability distributions 30
3.3 Results 34
3.4 Summary 35
4 Micro-Macro Entanglement Under General Coarse-grained Measurements 37
4.1 Method 38
  4.1.1 New measure-and-prepare cloner 38
  4.1.2 Probability distribution for measurements in an arbitrary basis . . 39
  4.1.3 Coarse-graining Model 40
  4.1.4 Measure for comparison 40
4.2 Results 41
4.3 Summary 43
5 Discussion and Conclusion 44
Bibliography 46
A Equatorial probability distributions 51
A.1 Probability distribution for PC-cloner 51
A.2 Probability distribution for PC-cloner 52

A.3 Measurements with non-zero $\Delta\phi$ 52
B General probability distributions 54
B.1 Probability distribution for PC-cloner 54
B.2 Probability distribution for MP-cloner 55
B.3 Graphs for general measurements 56

List of Tables

B.1 Statistical distance between PC-cloner and MP-cloner as a function of error and bin size for different angles. 56

List of Figures

2.1 Schematic of Bloch sphere. Bloch sphere represents the Hilbert space of a qubit which is parametrized by two angles. 15
2.2 The set-up of De martini's proposal. A singlet state is produced in a spontaneous parametric down conversionprocess. One photon goes to channel A and the the other photon is being amplified with the phase covariant cloner. 18

3.1 The figure on the left is the Schematics of De martini's experiment with quantum phase covariant cloner and the one on the right is the analugue set-up with classical measure-and-prepare cloner. 27
3.2 Probability distributions for classical and quantum mechanically amplified states for $\Delta\phi = 0$. The x-axis indicates possible out comes on detector B1 as in Figure [2.2] and the y-axis the probability of getting that outcome. 34
3.3 Coarse-Grained probability distributions. The x-axis indicates possible outcomes after coarse-graining and the y-axis indicates the probability of getting coarse-grained outcomes. 35

4.1 This graphs shows $D(j)$ as a function of the relative error $\frac{sigma}{N}$, for different value of N. As N increases, e.g. for $N \simeq 10^4$ the distance is expected to vanishes for even small inaccuracies. 42
4.2 This graphs shows $D(j)$ as a function of $2\sigma + 1$, the size of the bin, for different value of N. For large values of the bin size, the distance for different values of N decreases to the same value. 42

A.1 Coarse-grained probability distribution for $\Delta\phi = \pi$ with equatorial measurements 53

Chapter 1

Introduction

The question of why quantum effects are not present in our daily life, has been puzzling physicists since the early days of quantum mechanics.This question was first formulated by Schrödinger in 1935[5]. He proposed the idea of Schrödinger's cat which is a thought experiment that results in entanglement between a cat, as a macroscopic object, and the state of an atom.

One answer to the question of Quantum-to-Classical transition is that macroscopic systems do not evolve coherently: quantum mechanics transits to classical physics due to the interaction with the environment. This approach is called the decoehrence program [6, 7]. A famous example in this area is the cat-state. A cat state has the following form:

$$|\text{cat-state}\rangle = |\alpha\rangle + |-\alpha\rangle, \tag{1.1}$$

where $|\alpha\rangle$ is a coherent state. The Wigner function of a cat-state has some negative contribution in phase space which is a signature of non-classicality. But decoherence results in a diffusion process that makes positive and negative ripples interfere and cancel out. Consequently, the Wigner function of the cat-state after decoherence is similar to the classical picture.

Here I consider a complementary approach that puts the emphasise on the precision of measurements. In this approach, one can describe the Quantum-to-Classical transition for the cat-state above in terms of the precision of homodyne detection. Specifically, the resolution of measurements should be good enough to demonstrate ripples in phase space in order to manifest the non-classicality of cat-state. Note that this is not in contradiction with the decoherence program but is an alternative way of answering the Quantum-to-

Classical transition problem. In other words, this approach explains that even if one can keep the evolution coherent, one still needs precise measurements to see non-classicality.

This approach was exploited in [8] to explain the Quantum-to-Classical transition for spin dynamics. They showed that if measurements are strongly coarse-grained, the dynamics of quantum spin looks exactly like the classical spin.

An important example of Quantum-to-Classical transition problem is the transition from quantum entanglement to classical correlation. There have been attempts to bring entanglement to the macroscopic level. For instance, in [4], De Martini et al. claimed the generation of entanglement between a single photon and a macroscopic beam of light, which is visible with the naked eye.

In this thesis, I make a statistical comparison between the entanglement in this system and a classical correlation between the two parties involved. The result is that although the quantum entanglement in De Martini's experiment is different than a classical correlation, an extremely sophisticated experiment would be needed to show this difference. More specifically, one has to be able to count large number of photons with a resolution at the single photon level to demonstrate the entanglement. Otherwise quantum entanglement after coarse-graining is not different than classical correlation. Therefore, I report a Quantum-to-Classical transition for quantum entanglement that occurs under the constraint of coarse-grained measurements.

Chapter 2

Background

2.1 Entanglement

Entanglement is one of the key features of quantum mechanics that differentiate it from classical physics and provides a really useful resource for both understanding the fundamentals of nature and utilizing different technologies. This property was first recognized by Einstein, Podolsky, and Rosen (EPR) in their famous paper in 1935 [9]. It was also the first time that the fundamental non-classical aspect of quantum entanglement was identified. In the same year, Schrödinger did some further studies on the EPR state (the two particle state which was used in the EPR paper) and realized that it does not allow one to ascribe a state to individual particles.

In this section, I explain quantum entanglement and some criteria for its detection.

2.1.1 Definition

There is a fundamental difference between the description of physical systems in quantum mechanics and classical physics. In classical physics systems are described by points in a phase space, whereas in quantum mechanics systems correspond to vectors in a Hilbert space. For composite systems, this results in a gap. In phase space, the state of a composite system is described by the product of the states of individual components, but in a Hilbert space this description could in general be more complicated, i.e. superposition of product states. To clarify this point, consider the following quantum state:

$$|\Psi^-\rangle = \frac{|1,\, 0\rangle_{a,b} - |0,\, 1\rangle_{a,b}}{\sqrt{2}}. \tag{2.1}$$

This state is called a *singlet state.* It includes two sub-systems a and b and each of them could be either in state 1 or 0. The subscript a, b indicates that the first number is the state of system a and the second one is the state of system b, i.e. $|1,\, 0\rangle_{a,b} = |1\rangle_a \otimes |0\rangle_b$. One can easily see that there is no way to rewrite $|\Psi^-\rangle$ as a product state e.g. $|\Psi_a\rangle \otimes |\Psi'_b\rangle$. Such states are called *entangled states.* For pure quantum states, one can define an entangled state as a state that could not be described as a product of states of individual sub-systems.

For mixed states it is more complicated to define entangled states. In 1989 Werner defined separable states as a convex combination of product states [10]:

$$\rho = \sum_i p_i \rho_1^i \otimes \rho_2^i \cdots \otimes \rho_n^i, \tag{2.2}$$

where the system involves n subsystems. Werner defined a general entangled state as a state that is not separable.

One of the main questions that the theory of entanglement is trying to answer is how to detect entanglement. For different situations, different methods have been developed to deal with this problem.

Detection of entanglement is one of the main topics in my project. Therefore, I will explain the three methods for the detection of entanglement that are relevant for my work.

2.1.2 Detection of entanglement

There are different methods for the theoretical detection of entanglement. Usually these are based on necessary conditions for separability. For instance, if a state of a compound system is separable, then the partial transpose of its density matrix is a positive matrix. This was reported as a criterion for entanglement in 1996 by Peres [11].

Here I will introduce several criteria which are relevant to the context of micro-macro entanglement. These criteria distinguish multi-particle entangled states from separable ones.

Criteria 1

In 2003 C. Simon and D. Bouwmeester proposed a method to establish multi-photon entanglement. In the same paper, they derived a criterion for detection of entanglement in multi-particle states[12].

This criterion was derived for spin-like systems and although the primary motivation was for optical polarization qubits, there is an analogy between spin systems and polarization in optical systems based on Stokes polarization vectors. Mathematically, for the polarization of photons, spin is defined as:

$$
\begin{aligned}
J_x &= \frac{a_+^\dagger a_+ - a_-^\dagger a_-}{2}, && (2.3)\\
J_y &= \frac{a_l^\dagger a_l - a_r^\dagger a_r}{2}, && (2.4)\\
J_z &= \frac{a_h^\dagger a_h - a_v^\dagger a_v}{2}. && (2.5)
\end{aligned}
$$

Here a_h, a_v represent horizontal and vertical polarizations, a_+, a_- represent the ±45 polarizations and a_l, a_r represent the left- and right-handed polarizations. These operators correspond to Stokes parameters of polarization. One can show that:

$$\langle \hat{J}^2 \rangle = \langle J_x^2 \rangle + \langle J_y^2 \rangle + \langle J_z^2 \rangle = \frac{N}{2}(\frac{N}{2} + 1). \qquad (2.6)$$

The parameter N is the total number of the photons and equals $a_h^\dagger a_h + a_v^\dagger a_v$.

For a bipartite system with sub-systems A and B, the criterion is that for any separable state, the following inequality holds:

$$\frac{\langle J^2 \rangle}{\langle N \rangle} \geq \frac{1}{2}, \qquad (2.7)$$

where $\vec{J} = \vec{J}_A + \vec{J}_B$ is the total angular momentum and $N = N_A + N_B$ is the total number of particles. To prove Eq. [2.7], they start with the expectation values on a general separable state like Eq. [2.2]. That is $\rho = \sum_i p_i \, \rho_A^i \otimes \rho_B^i$. Their proof is as follows:

$$\begin{aligned}\langle J^2 \rangle &= \langle J_A^2 \rangle + \langle J_B^2 \rangle + 2\langle J_A .\, J_B \rangle \\ &= \sum_i p_i \left[\langle J_A^2 \rangle_i + \langle J_B^2 \rangle_i + 2\langle J_A \rangle_i . \langle J_B \rangle_i \right] \\ &\geq \sum_i p_i \left[\langle J_A^2 \rangle_i + \langle J_B^2 \rangle_i - 2 \left| \langle J_B \rangle_i \right| \, \left| \langle J_B \rangle_i \right| \right], \end{aligned} \tag{2.8}$$

where $\langle J_A \rangle_i = Tr \rho_i^A J^A$, etc. On the other hand, $|\langle J \rangle| \leq \sqrt{\langle J^2 \rangle + \frac{1}{4}} - \frac{1}{2}$. They define $\alpha = \sqrt{\langle J_A^2 \rangle + \frac{1}{4}} - \frac{1}{2}$ and $\beta = \sqrt{\langle J_B^2 \rangle + \frac{1}{4}} - \frac{1}{2}$. This simplifies the Eq. [2.8] to:

$$\geq \sum_i p_i \left[\alpha_i^2 + \alpha_i + \beta_i^2 + \beta_i - 2\alpha_i \beta_i \right] = \sum_i p_i \left[(\alpha_i - \beta_i)^2 + \alpha_i + \beta_i \right] \geq \sum_i p_i \left[\alpha_i + \beta_i \right] \tag{2.9}$$

On the other hand as $J^2 = \frac{N}{2}(\frac{N}{2} + 1)$,

$$\alpha = \sqrt{\langle J_A^2 \rangle + \frac{1}{4}} - \frac{1}{2} = \sqrt{\frac{N_A}{2}(\frac{N_A}{2} + 1) + \frac{1}{4}} - \frac{1}{2} = \sqrt{(\frac{N_A}{2} + \frac{1}{2})^2} - \frac{1}{2} = \frac{N_A}{2}. \tag{2.10}$$

This completes the proof as:

$$\langle J^2 \rangle \geq \sum_i p_i \left[\alpha_i + \beta_i \right] \geq \frac{1}{2} \langle N_A + N_B \rangle = \frac{1}{2} \langle N \rangle \rightarrow \frac{\langle J^2 \rangle}{\langle N \rangle} \geq \frac{1}{2}. \tag{2.11}$$

Later in [13, 14] P. Sekatski et al. built up on the Eq. [2.11] and derived the following inequality for separable states.

$$|\langle J_A .\, J_B \rangle| \leq \langle N_A N_B \rangle. \tag{2.12}$$

For the proof see [14].

Criteria 2

H. S. Eisenberg et al. in 2004 presented a criterion for separability[15]. This is a criterion for bipartite systems with 2-dimensional Hilbert spaces.

The total spin-correlation $\langle \overrightarrow{\sigma^a} \,.\, \overrightarrow{\sigma^b} \rangle$ for a separable system should satisfy the following inequality:

$$\left| \langle \overrightarrow{\sigma^a} \,.\, \overrightarrow{\sigma^b} \rangle \right| = \left| \langle \sigma_x^a \,.\, \sigma_x^b \rangle + \langle \sigma_y^a \,.\, \sigma_y^b \rangle + \langle \sigma_z^a \,.\, \sigma_z^b \rangle \right| \leq 1. \tag{2.13}$$

This is because for separable states, the magnitude of the total spin-correlation is maximum when the two spins are parallel or anti-parallel. One can simply rotate each spin to the z-axis in which case the maximum total spin-correlation would be equal to one. This introduces a condition on separable states. If this inequality is violated for a state, that state is entangled. For instance consider the state in Eq. [2.1]: the spin-correlation for that bipartite state is maximum in all directions, meaning that the total correlation is three. This violates the inequality of Eq. [2.13], so the state should be entangled.

Note that this criteria could be similarly used for polarization qubits.

Criteria 3

Recently N. Spagnolo et al. in [16] found a new separability criterion for multi-photon entanglement. Their goal was to demonstrate the entanglement for the experiment in [4] and they needed a criterion similar to the one introduced in Eq. [2.1.2] but for multi-photon qubits.

In De Martini's experiment they wanted to demonstrate the entanglement between a single photon and a multi-photon beam of light. When loss is present, the macro-qubit is not a perfect qubit and lives in a high-dimensional space rather than a 2-dimensional Hilbert space. Therefore they can not use the criterion in Eq. [2.7] and they presented a new one.

The criterion is that:

$$S = \langle \sigma_1^a \otimes D_1^b \rangle + \langle \sigma_2^a \otimes D_2^b \rangle + \langle \sigma_3^a \otimes D_3^b \rangle \leq \sqrt{3}, \tag{2.14}$$

where D_i is a set of diatomic operators and a and b represent the two sub-systems. The proof is similar to the one for Section 2.1.2. For more information see [16].

These criteria are being used frequently in the context of micro-macro entanglement. In Section 2.3.1 I will explain more about the applications.

The other concept which should be explained before I proceed to the micro-macro entanglement is quantum cloning. My main focus here is, first, on the fundamental limitations on quantum cloning and then on the physical realization of different cloning methods. The next section will address these two subjects.

2.2 Quantum cloning

Quantum cloning was first explored in 1982, in the context of superluminal communication [17]. The idea is to share a pair of photons, which is in a singlet state, between *Alice* and *Bob*. *Alice* performs a measurement in some basis on her pair. This projects *Bob* system onto the state orthogonal to *Alice*'s state. If *Bob* could find out what state he has, he could infer what measurements *Alice* performed. On the other hand, if he could perfectly clone his state, he could do a tomography on his state and he would learn his state. That means, with perfect cloning, *Bob* would be able to infer *Alice*'s measurement and if this is being done fast enough, it could be used for superluminal communication between *Alice* and *Bob*. Herbert proposed this idea in [17] and suggested a physical realization of cloning based on stimulated emission.

This idea connected the two concepts of quantum cloning and quantum no-signaling.

In fact, Herbert found that perfect cloning results in superluminal quantum signaling.

On the other hand, it was proved that superluminal communication is not possible in quantum mechanics [18]. This apparent contradiction was resolved by the quantum no-cloning theorem in 1982 by Wotters and Zurek. They proved that due to the linearity of time evolution operators in quantum mechanics, perfect cloning is not possible[19]. It also was proved that due to unavoidable spontaneous emissions, the stimulated emission could not create perfect copies and it is impossible to realize the perfect-cloning with stimulated emission[20, 21].

Then the idea of approximate cloning was introduced in [22] and the optimal bound on that was found[23]. I will explain this concept in more detail in Section 2.2.2.

In my work, quantum cloning plays an important role. I exploit quantum cloners to amplify the quantum effect of entanglement to a macroscopic level.

In this section, I will overview some basic elements of quantum cloning. I will start with illustration of the quantum no-cloning theorem. Then I will explain the concept of approximate cloning in Section 2.2.2 and at the end, in Section 2.2.3, I will introduce some cloning methods that are relevant to my work.

2.2.1 No-cloning theorem

After Herbert published his paper, in the same year, Wootters and Zurek realized that there was a problem with Herbert's work[19]. In fact, the linearity of operations in quantum mechanics does not allow for perfect coping. Mathematically, this cab be shown in the following way. Let's consider U as copying machine for a qubit system. That means:

$$U|\psi\rangle_s|0\rangle_t|0\rangle_e = |\psi\rangle_s|\psi\rangle_t|f_\psi\rangle_e. \tag{2.15}$$

The $|\psi\rangle_s$ is the source state to be copied. The $|0\rangle_t$ is the target which is initially in $|0\rangle$ and after applying U, should transform to a copy of the source qubit. The $|0\rangle_e$ represents the state of the environment. Now let's consider the action of copying machine on $|+\rangle = \frac{|0\rangle+|1\rangle}{\sqrt{2}}$. There are two ways to apply U on the state. One can first apply it on the state itself which results in:

$$|+\rangle_s|0\rangle_t|0\rangle_e \to |+\rangle_s|+\rangle_t|f_+\rangle_e. \tag{2.16}$$

On the other hand, as U is a quantum mechanical evolution, it should be unitary. That means:

$$\begin{aligned} U|+\rangle_s|0\rangle_t|0\rangle_e &= U(\frac{|0\rangle_s+|1\rangle_s}{\sqrt{2}})|0\rangle_t|0\rangle_e \\ &= (\frac{U|0\rangle_s+U|1\rangle_s}{\sqrt{2}})|0\rangle_t|0\rangle_e = \frac{|0\rangle_s|0\rangle_t|f_0\rangle_e+|1\rangle_s|1\rangle_t|f_1\rangle_e}{\sqrt{2}}. \end{aligned} \tag{2.17}$$

One can easily see that Eq. [2.16] and Eq. [2.17] could not be identical which means that copying are not be done unitarily.

2.2.2 Approximate cloning

In 1996, Bužek and Hillery came up with a different idea[22]. Instead of a perfect cloner, they considered a cloning machine which produces approximate clones. One can quantify this in terms of fidelity. Fidelity is a measure that quantifies closeness between two states. For instance for the distance between two density matrices, σ and ρ, the fidelity is defined as:

$$F(\sigma,\rho) = \left(Tr\sqrt{\sqrt{\sigma}\rho\sqrt{\sigma}}\right)^2 \tag{2.18}$$

For more information see [24].

In this language, perfect cloning means that the fidelity between the source state and targets is one. An approximate cloning machine produces clones which are not necessarily as good and their fidelities are less than 1.

In [22], Bužek and Hillery propose a 1 to 2 cloner. Their cloning transformation was:

$$|0\rangle_s|0\rangle_t|0\rangle_e \rightarrow \sqrt{\frac{2}{3}}|0\rangle_s|0\rangle_t|1\rangle_e + \sqrt{\frac{1}{6}}(|1\rangle_s|0\rangle_t + |0\rangle_s|1\rangle_t)|0\rangle_e, \tag{2.19}$$

$$|1\rangle_s|0\rangle_t|0\rangle_e \rightarrow \sqrt{\frac{2}{3}}|1\rangle_s|1\rangle_t|0\rangle_e + \sqrt{\frac{1}{6}}(|1\rangle_s|0\rangle_t + |0\rangle_s|1\rangle_t)|1\rangle_e. \tag{2.20}$$

The fidelity of the clones in this method is $\frac{5}{6}$ which was proved to be optimal[23].

Gisin and Massar in [25] generalized the idea in [22] to cloning from N inputs to M copies. They also proved that their cloning machine is optimal [23].

In 1998, Bruss et al. derived a general upper-bound for any type of approximate cloning machine[23]. Their idea was based on the connection between quantum state estimation and quantum cloning. One way to estimate a state is to clone it and then do a tomography on clones. With this process, the optimal fidelity of clones could not exceed the optimal upper bound for state estimation. These bounds are based on the best possible estimation that could be achieved having M copies of the state.

On the other hand, state estimation could be exploited to make a cloning machine. Specifically, one can estimate the state first and then produces copies of that state. In this case, the optimal fidelity for state estimation could not be greater than the upper bound on the optimal fidelity of state cloning. This means that the upper bound on the optimal fidelity of quantum state estimation is the same as quantum cloning.

Using this idea, the optimal fidelity is:

$$F = \frac{NM + M + N}{M(N+2)}. \tag{2.21}$$

This upper-bound is saturated by Buže-Hillery and Gisin-Massar cloning machines.

Note that in the cloning methods introduced by Bužek-Hillery and Gisin-Massar, the fidelity is the same for all inputs. These type of cloners are called *universal cloners.* Not all cloners are universal. For instance, the phase covariant cloner which will be introduced in Section 2.2.3 is not universal and produces better clones for state on the equator of Bloch sphere. Bloch sphere is a geometrical representation of Hilbert space of 2-level quantum systems. See Figure [2.1].

In the next section, I will introduce three types of cloning methods that are relevant to my work. I will also describe how they could be realized experimentally.

2.2.3 Physical realization of different cloning machines

Universal cloner

As mentioned before, a universal cloning machine (UCM) produces clones that are equally good for any input qubit. More specifically, for any qubit on Bloch sphere, the fidelity of clones that a universal cloning machine produces is the same.

The optimal asymptotic fidelity for such a cloning machine is $\frac{2}{3}$. An interesting question is whether or not, one can achieve this optimal bound in experiment. In [26], Simon et. al. proposed two methods based on the stimulated emission for this purpose; I will describe the second method which is based on stimulated parametric down conversion process. This is an optical process and qubits are defined as the polarization of photons. This process could be realized using a non-linear crystal type II.

In this process, in addition to the source qubit, a pump laser is incident onto the non-linear crystal. The effective Hamiltonian on the input qubit becomes:

$$H = i\chi(a_h^\dagger c_v^\dagger - a_v^\dagger c_h^\dagger) + H.c., \tag{2.22}$$

where χ is proportional to non-linear susceptibility of the crystal and the intensity of the laser pump, a is the input mode which is to be cloned and c is the environment mode. The universal cloning machine produces some photons in the environment mode which are traced out. These photons are called anti-clones. Therefore, the universal cloning is not a unitary process if one just considers clones.

One can show that this Hamiltonian is invariant under joint rotations of a and c which is $e^{-i\hat{\theta}.\hat{J}}$. Due to this symmetry, the fidelity of clones is independent of input photons.

Phase covariant cloner

This type of cloner produces clones that are equally good for states on the equator of Bloch sphere. That means for equatorial qubits, fidelity is constant. This type of cloning was first introduced in [27]. In the same paper, Bruß et al. found an upper-bound on the fidelity for the optimal phase covariant cloners with a similar method to [23]. They also show that the fidelity of phase covariant cloning is more than the fidelity for universal cloning machine. For cloning one qubit into M clones, the asymptotic fidelity is 3/4. This is reasonable as cloning a specific group of qubits from Bloch sphere is easier and better than cloning for all qubits. In the extreme case, if one confines the cloner to just clone a specific qubit $|0\rangle$, then it can be cloned perfectly but at the cost of poor fidelity for other states like $|+\rangle$.

Optimal phase covariant cloner was first physically realized in [28] for $1 \to 3$. In that paper, Sciarrino and De Martini exploited a $1 \to 2$ universal cloner, a not gate and a projection onto the symmetric sub-space for this purpose.

Later a different method of phase covariant cloning was introduced for polarization of photons in [29]. It was based on using an optical amplification. This method is similar to the universal cloning machine. The source photon with a strong pump of a pulsed Ultra Violet (UV) laser is fed into a non-linear crystal. The effective interaction between the source photon and the optical amplifier is described by the following Hamiltonian:

$$H = i\chi a_h^\dagger a_v^\dagger + H.c.\,, \tag{2.23}$$

where χ is proportional to non-linear susceptibility and the intensity of the pump of laser. In this method there is no anti-clone and all the photons remain at the end. That means if there is no loss, this process is a unitary evolution.

In order to see that this evolution is symmetric under rotations on the equator of Bloch sphere, one can rewrite the Hamiltonian as:

$$H = i\chi(\left(a^\dagger_\phi\right)^2 + \left(a^\dagger_{\phi\perp}\right)^2) + H.c., \tag{2.24}$$

where $a^\dagger_\phi$ and $a^\dagger_{\phi\perp}$ represent the creation operators for the photons on the equator at angle ϕ and $\phi + \pi$ respectively. Figure [2.1] shows these polarization vectors on Bloch sphere. The two points on poles indicates horizontally and vertically polarized photons.

A general state $|\psi\rangle$ on Bloch sphere is represented by two angles, θ and ϕ as in Figure [2.1]. I use the following notation for such a state:

$$|\psi\rangle = |\theta, \phi\rangle. \tag{2.25}$$

Occasionally if the state is on the equator, I drop the θ for simplicity. Similarly, $|n\rangle_{\theta,\phi}$ represents a multi-photon state with n photons in $|\theta, \phi\rangle$. The state orthogonal to $|\psi\rangle$ is denoted by:

$$|\psi^\perp\rangle = |\theta, \phi\perp\rangle. \tag{2.26}$$

These two states make a basis. A general pure state with N photons in this basis is represented by $|j, N-j\rangle_{\theta,\phi} = |j\rangle_{\theta,\phi} \otimes |N-j\rangle_{\theta,\phi\perp}$ where j is the number of photons in the state corresponding to $|\theta, \phi\rangle$.

Eq. [2.24] holds for any angle ϕ and this means the Hamiltonian is symmetric for all equatorial angles, ϕ. Due to this symmetry, the fidelity for all input states on the equator is the same.

This cloner plays an important role for the amplification of entanglement in [4]. I will discuss this in more detail in Section 2.3.1.

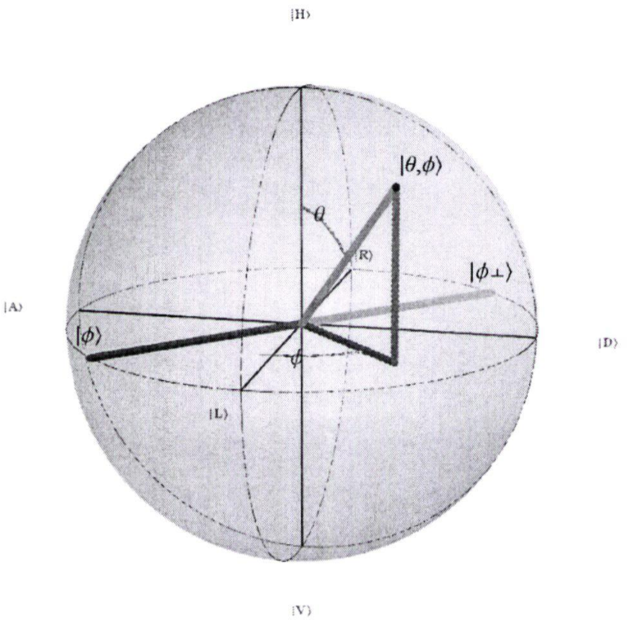

Figure 2.1: Schematic of Bloch sphere. Bloch sphere represents the Hilbert space of a qubit which is parametrized by two angles.

Measure-and-Prepare cloner

As discussed before, an other way of cloning is to simply measure the state of the source qubit and create copies of them. More specifically, a measure-and-prepare cloning machine measures the state of the input qubit in some random basis and produces M photons in the state corresponding to the measurement outcome. Mathematically, the density matrix after cloning with this method is:

$$\rho_{mp} = \frac{1}{\pi} \int d\phi_{mp} (P^{+}(\phi_{mp}) \mid \Phi_{\phi_{mp}} \rangle \langle \Phi_{\phi_{mp}} \mid + P^{-}(\phi_{mp}) \mid \Phi_{\phi_{mp}\perp} \rangle \langle \Phi_{\phi_{mp}\perp} \mid), \qquad (2.27)$$

where $P^{\pm}(\phi_{mp})$ indicates the probability of getting $\pm$ outcome for the measurement and the state $\mid \Phi_{\phi_{mp}} \rangle$ is the state, involving N photons, that the cloner generates if the measurement outcome in $\{\phi_{mp}, \, \phi_{mp} \perp\}$ basis on the single photon is ϕ_{mp}.

For input state $\mid \psi_{in} \rangle = |1, 0\rangle_{\frac{\pi}{2}, \phi_{in}}$, probabilities are:

$$P^{+}(\phi) = \cos\left(\frac{\phi}{2}\right), \quad P^{-}(\phi) = \sin\left(\frac{\phi}{2}\right). \tag{2.28}$$

This introduce a class of cloners. One can adjust the measurement and the generated state to design any arbitrary amplifier. For the purpose of this work, I need a phase covariant cloner and I confine the generated state to:

$$| \Phi_{\phi}\rangle = |N\rangle_{\phi} = \frac{\left(a_{\phi}^{\dagger}\right)^{N}}{\sqrt{N!}}|0\rangle. \tag{2.29}$$

Due to the integration over all equatorial angles or more physically, because of random measurements in all bases on the equator, this type of measure-and-prepare cloner is phase covariant. One can simply show that for $N \to \infty$, this cloner is also optimal for all states on the equator. That means the fidelity of clones on the equator goes to $\frac{3}{4}$. This cloner has been introduced before in [14]. Note that this is not the general measure-and-prepare cloner, but is the cloner I will use in Chapter 3. Later in Chapter 4 I will modify the state of Eq. [2.29].

It is known that the process of measurement breaks entanglement. That means if two particles are entangled, a measurement on any of the two particles reduces the compound state into a separable state. As there is a measurement in the measure-and-prepare cloning process, any quantum correlation between the source qubit and other systems is broken after the cloning. In other words, after the measure-and-prepare cloning, clones could only be classically correlated with other systems. This provides me with a powerful tool to generate micro-macro systems with pure classical correlation. Later in Section 3.2.1, I will exploit this cloner to produce some classical correlation that approximates the quantum correlation in De Martini's experiment.

2.3 Micro-Macro entanglement

Experimental establishment of entanglement has always been one of the most fascinating problems in quantum physics. This becomes even more interesting when it gets to the macroscopic level. Establishment of entanglement between macroscopic objects or even micro- and macro- systems is of special interests in quantum physics[1, 2, 3]. Not only it does improve our understanding of quantum physics, but it also provides us with a powerful tool to study some fundamental aspects of nature e.g. macro realism[30].

In recent years there has been substantial effort for establishment of macro-entanglement, and consequently there has been a significant progress in this area. Right now, there are different proposals for producing macroscopic entanglement e.g. superconducting qubits [1], opto-mechanical qubits [2] and combination of superconducting qubits and mechanical systems[3]. One of the most promising ones is an experiment by De Martini et al. in [4]. They used an optical set-up and they considered photons as their systems. They have reported experimental establishment of entanglement between polarization of one single photon and polarization of photons in a macro-beam of light, although the claim to have demonstrated entanglement was subsequently challenged, see below. Here I explain this experiment in detail.

2.3.1 Micro-Macro entanglement in optical systems

C. Simon et al. in [12] proposed the idea of using the parametric down conversion process for creation of multi-photon entanglement in polarization of light. The following year, this proposal was exploited by HS. Eisenberg et al. in [15] to establish bipartite multi-photon entanglement. In their experiment, they used two criteria to demonstrate the entanglement between up to 12 photons. This was the first time that entanglement was established for such a relatively large large number of photons.

Recently, in 2008, De Martini et al. took the next step and for the first time, they

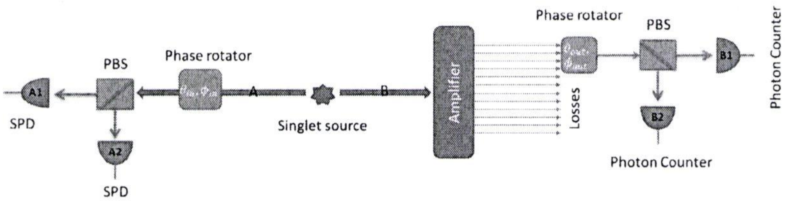

Figure 2.2: The set-up of De martini's proposal. A singlet state is produced in a spontaneous parametric down conversionprocess. One photon goes to channel A and the the other photon is being amplified with the phase covariant cloner.

claimed establishment of entanglement between a single photon and a beam of light which is visible to the naked eye[4]. P. Sekatski et al. in [13] showed that this beam of light is in principle macroscopic enough to violate the Bell-inequality with naked eye. More precisely, they showed that one can use the naked eye as a detector for the beam of light, and correlations between measurement results on the single photon and measurement results with the eye violate a Bell inequality.

In this section, I explain their experiment in detail and then I describe the method they use to demonstrate the entanglement. This method relies on strong assumptions which were analysed later in [14] and [16] and will be discussed in more detail below.

De Martini's experiment

They start with an entangled pair of photons in the singlet state, $|\Psi^-\rangle = 1/2(|R\rangle_A|L\rangle_B - |L\rangle_A|R\rangle_B)$ which is produced in a spontaneous parametric down conversion process. Here $\{\ |R\rangle$ and $|L\rangle\ \}$ indicate right- and left-handed polarizations. See Figure [2.1] for more detail.They implement this process using a non-linear crystal pumped by a pulsed UV laser. One photon goes to channel A and is subsequently measured. The other photon is being amplified through a phase covariant cloner to a macroscopic state. Figure [2.2] shows a schematic of their experiment.

De Martini used the cloning method proposed in [29] which is based on a process called quantum injected optical parametric amplification. This is a unitary transformation which takes a single photon and a pump beam to a macro-qubit which involves about $N \approx 10^4$ number of photons. They used a non-linear crystal with a laser pump to implement it. The effective evolution on the input photon is a parametric down conversion process with the Hamiltonian of Eq. [2.23] which is $H = i\chi a_h^\dagger a_v^\dagger + H.c.$.

The singlet state can be rewritten as:

$$|\Psi^-\rangle = 1/2(|\phi\rangle_A|\phi^\perp\rangle_B - |\phi^\perp\rangle_A|\phi\rangle_B), \tag{2.30}$$

where $|\phi\rangle = |\frac{\pi}{2}, \phi\rangle$ represents the equatorial state at angle ϕ. Then the state after the amplification on channel B can be written as:

$$|\Sigma\rangle_{A,B} = 2^{-1/2}\left(|\Phi^\phi\rangle_B|\phi^\perp\rangle_A - |\Phi^{\phi\perp}\rangle_B|\phi\rangle_A\right), \tag{2.31}$$

where $\{|\Phi^\phi\rangle, |\Phi^{\phi\perp}\rangle\}$ are orthogonal macroscopic states after the amplification. As they are orthogonal, the state $|\Sigma\rangle$ is a macro singlet state. I will derive the explicit form of this state in Section 3.2.2.

After the amplification they split the macro-beam into two orthogonal polarizations, e.g. $|R\rangle \& |L\rangle$. The number of counted photons is translated to two currents, $\{I_R, I_L\}$. If the difference between the two currents exceeds some threshold, the measurement counts as a conclusive one. Otherwise, it is ignored. For instance if $I_R - I_L > k$, where k is the threshold, then it means that the output state was corresponding to $|R\rangle$. If $I_L - I_R > k$ then the beam of light is in the state corresponding to $|L\rangle$. But if $|I_R - I_L| < k$, this is not a conclusive measurement and this would be ignored. Finally they study the correlation between the measurement outcome on the single photon of channel A and the macro-beam of light.

Those set of measurements for which $|I_R - I_L| < k$ implies some post-selection on De Martini's measurements which opens up a loophole in their experiment[14, 16].

Demonstration of entanglement

De Martini et al. in [4] used the criterion in Eq. [2.13] and reported the demonstration of entanglement for the extremely coarse grained measurement that was explained above. Their demonstration of entanglement is based on the fact that the average number of photons for the polarization mode corresponding to ϕ is $\sinh^2 g$ for $|\Phi^{\phi\perp}\rangle_B$, and $(3\sinh^2 g + 1)$ for $|\Phi^{\phi}\rangle_B$ and for the polarization mode $\phi \perp$ is $\sinh^2 g$ for $|\Phi^{\phi}\rangle_B$, and $(3\sinh^2 g + 1)$ for $|\Phi^{\phi\perp}\rangle_B$. Therefore if the difference between the counted number of photons in the orthogonal basis is greater than some threshold, they can distinguish the output state. But there also some cases where the outcome is not conclusive, resulting in some post-selection which, opens up the detection loophole. It is also extremely coarse-grained because the resolution on photon-counting measurement does not really matter.

In [13], P. Sekatski et al. used criterion 1 as in Eq. [2.7] and they showed that theoretically there is entanglement between the single photon on channel A and the beam of light on channel B even if the loss after amplification is taken into account. They found that:

$$\left|\langle \vec{J^a} . \vec{J^b}\rangle\right| - \langle N^a\rangle = 2\eta, \tag{2.32}$$

where η is the transmission rate of detection process. Even in the ideal case when $\eta = 1$, the difference is no more than 2 which means almost perfect photon counting measurements are required to demonstrate the entanglement experimentally using this method. In other words, if counted number of photons is inaccurate by even 2 photons out of 10^4 photons, then it is not likely to demonstrate entanglement. This motivated my work, as I want to see if it is possible to demonstrate entanglement under coarse-grained measurements.

According to Eq. [2.7] the state would be separable only when there is no transmission and even for high losses through the process, there still would be entanglement in the system. Note that this is just the loss in the detection process and it does not include losses in the amplification process. Losses in amplification process was considered in [14] and it is more complicated. Currently there is no theoretical proof for entanglement if there is loss in the amplification process.

In [14] P. Sekatski et al. showed that the demonstration method that De Martini used fails for some separable states. In fact, the criterion that De Martini et al. used, report some separable states as entangled [14, 16]. There are two issues with their demonstration method: the criterion that they used, is designed for a bipartite system with 2-dimensional Hilbert spaces where considering the loss, the macro-qubit lives in a higher dimensional Hilbert space; as well, post-selections in their experiment opens up the detection loophole.

Later, in 2010, Spagnolo et al. in [16] stated that with some supplementary assumption it still is possible to infer the result of [4] as a demonstration of entanglement. Their supplementary assumption was that if one knows that the micro-macro correlation is produced with a quantum cloner e.g. parametric down conversion process, then the demonstration method used in [4] is conclusive. This still is assuming that there is no loss before and during the amplification process.

In the same paper, they propose a different method for demonstration of entanglement which is based on attenuation. This method was exploited before in [15, 31]. They consider a high loss channel such that most photons of the macro qubit on channel B are lost. Then only a single photon is left and they can use their criterion safely for that single photon, because after the loss, it would be a two-dimensional qubit system. They demonstrate entanglement between two single photons. Demonstration of the entanglement after attenuation means that there was entanglement before that, because entanglement dose not increase under local operations [32] and attenuation is a local operation.

But the question is still open whether or not, one can demonstrate entanglement with coarse-grained measurements. That is what my project is addressing. The following section will explain in more detail what the idea beneath my project is.

2.3.2 My project

As explained above, there is a chance that the statistics of the micro-macro entanglement in the set-up presented in [4] could be reproduced with classical correlation between a single photon and a beam of light. I will show that, with even small inaccuracies in photon counting measurements, the statistics of De Martini's experiment could well be approximated with a classical correlation. This means that with even small imperfection in measurements, quantum correlation appears to be classical.

Here I consider the photon counting for the measurements as De Martini did in their experiment. Then I model imperfections by coarse-graining the photon number and show that coarse-graining results in a Quantum-to-Classical transition from entanglement to classical correlation. . This is not the first time that coarse-graining results in Quantum-to-Classical transition. Indeed, there is a proposal that explains Quantum-to-Classical transition for spin system in terms of coarse-grained measurements. In the next section I will explain more about this approach and one of the successful example in this picture.

2.4 Classical-to-Quantum transition and coarse-grained measurements

It has always been of special interest to understand the transition between classical and quantum mechanical physics. Here I will explain a viewpoint which is conceptually different than the decoherence program [6, 7] and collapse models[33, 34].

This approach is fully quantum mechanical which means it does not modify the theory of quantum mechanics but still explains why it is so rare to see quantum phenomena at the macroscopic level. More specifically, this viewpoint explains that due to limited precision of measurements in the lab, quantum effects transit to classical effects.

Currently there are some evidences which suggest that, this lack of precision for measurements could be a fundamental limitation in nature[35]. In this section, I will present a recent works which exploited the idea of coarse-graining for explanation of Quantum-to-Classical transition in spin systems. Then I will describe how I will use this idea in my own work.

2.4.1 Coarse-graining in spin system

In [8], J. Kofler and C. Brukner showed that for a spin system, coarse-graining could result in Quantum-to-Classical transition. They first showed that Leggett-Garg[36, 30] inequality, which is a macroscopic version of Bell inequality, is violated for even macroscopic systems if resolution for measurements of J_z is perfect. Then they show that in macroscopic level, when the resolution of measurements is not perfect, one cannot violate the macro-realism, i.e. Leggett-Garg inequality. Furthermore, they showed that in this case, the dynamics of this system, emerges to follow classical dynamics. Here I explain in more detail what they show.

They consider a system of spin j with an effective Hamiltonian like:

$$H = \omega \hat{J}_x. \tag{2.33}$$

This is the interaction for spin precession with frequency ω. They calculate the temporal correlation function of $Q = e^{i\pi(j-J_z)}$, which is the parity operator. The parameter j is the spin length. They define a macroscopic system as a system with large Hilbert space dimension which in this case is $2j + 1$.

The temporal correlation is defined as:

$$K = C_{12} + C_{23} + C_{34} - C_{14}, \tag{2.34}$$

where $C_{ij} = \langle Q(t_i)Q(t_j)\rangle$ is the temporal correlation function of operator Q. Legget-Garg inequality states that if macro-realism is true then:

$$K \leq 2. \tag{2.35}$$

They found that:

$$K \approx \frac{3\sin x}{x} - \frac{\sin 3x}{3x}, \tag{2.36}$$

where $x = (2j + 1)\omega\Delta t$ and Δt is the time distance in calculation of the temporal correlation. For x=1.054 the Leggett-Garg inequality is violated. This violation is independent of j which means no mater how macroscopic the system is, as far as the experiment resolution for Q is perfect, the inequality is violated.

They also show that for large j, if the accuracy in the measurement is not enough to resolve different eigenstate of j_z, then the dynamics of the system is effectively similar to the one for classical spin.

This suggests that classical dynamics could emerge from quantum dynamics when measurements are not accurate enough and coarse-graining could result in a Quantum-to-Classical transition. Later in 2010, Kofler et al. [35] provided some evidences that coarse-graining could be a fundamental limitation for spin systems. Their statement is based on the Heisenberg uncertainty principle combined with relativistic causality and finiteness of resources to show that for the macroscopic spin system above, the precision of measurements is fundamentally limited by laws of Nature.

2.4.2 Coarse-graining in De Martini's experiment

Precision for photon counting experiments is limited by current technology. Currently, the resolution of large photon counting is limited. In this thesis, I present a result similar to the one in [8] although there are some differences. For instance, the macroscopic system that I consider here, is a macro-beam of light which is observable with naked eye [13], where in [8] they define a macro-system as any system with a high dimensional Hilbert space. The other difference is that my focus here is on emergence of classical correlation out of quantum correlation, where in [8], they illustrated Quantum-to-Classical transition for the dynamics of the spin. In other words, here I consider quantum correlation as a quantum phenomena that has no classical analogue rather than the quantum dynamics which was considered in [8]. Finally, the result is that for photon counting measurements, coarse-graining results in a transition from quantum entanglement to classical correlation.

In the next Chapter I will explain in more detail how I study the correlation in De Martini's experiment, how I model the coarse-graining in photon counting measurements, and how classical correlations can approximate quantum entanglement.

Chapter 3

Micro-Macro Entanglement Under Equatorial Coarse-grained Measurements

In this chapter, I will explain how micro-macro entanglement in De Martini's experiment may be demonstrated when measurements are perfectly precise. On the other hand, I will show that demonstration of entanglement for De Martini's experiment is impossible without supplementary assumptions, if there are even small inaccuracies in the photon counting measurements. In other words, considering the limited precision of experiments, the entanglement between the single photon and the macro-beam of light becomes empirically indistinguishable from classical correlations. This suggests that coarse-graining may result in a Quantum-to-Classical transition.

In this chapter I focus on equatorial measurements for both the single photon and the beam of light. That is because the demonstration in [4] was proposed for equatorial measurements. Later in Chapter 4 I will extend this idea to general measurements.

In Section 3.1, I will explain the problem that I am considering. Then in Section 3.2, I will describe the method I am using in this work. Finally my results are presented in Section 3.3.

3.1 Problem

The system I am considering in this work was proposed by De Martini et al. in [4] and I explained it in detail in Section 2.3.1. As in Figure [3.1], there are two parties involved in this system. I am interested in the correlation between the two parties. More specifically, I would like to know if there is entanglement between the single photon on channel A

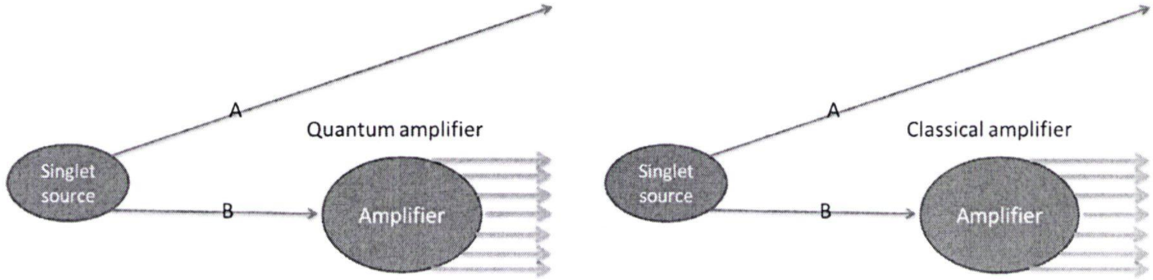

Figure 3.1: The figure on the left is the Schematics of De martini's experiment with quantum phase covariant cloner and the one on the right is the analugue set-up with classical measure-and-prepare cloner.

and the beam of light on channel B and, if there is, whether one can demonstrate this entanglement experimentally.

As discussed in Section 2.3.1, when there is no loss in the amplification process, there is entanglement between the micro-macro parties[13]. However in a real experiment, there are losses. In Section 2.3.1 I explained that when there is loss only after amplification, there is a theoretical proof of entanglement which requires sophisticated measurements for demonstration of entanglement. The number of photons must be counted almost exactly and for technical reasons, this precision is limited in measurements. Now the question is whether I can still demonstrate entanglement when there is inaccuracy in the outcomes and measurements become coarse-grained. This leads me to the main question of my work.

Problem 1: If photon counting measurements in De Martini's experiment are not accurate, assuming no other experimental imperfection, can one still demonstrate entanglement experimentally?

Here I show that, with even small inaccuracies in the measurements , it is almost impossible to observe the micro-macro entanglement. This could explain why it is hard to see Schrödinger's cat. Note that my goal here is not to do the experiment, but I examine experimental outcomes and losses from a theoretical viewpoint.

3.2 Method

To answer the question in Section 3.1, I propose an alternative question: How much does the quantum entanglement in De Martini's experiment differ from classical correlation? In other words, how closely can one approximate the quantum entanglement in De Martini's experiment with classical correlations? If classical correlation can approximate the quantum entanglement in this system after coarse-graining, then experimental demonstration of entanglement is impossible. For this approach, two ingredients must be specified; first, what the classical correlation is and second, how to model the noise and loss in the experiment.

For the classical correlation, I use the method introduced by P. Sekatski et al. in [14]. They simply replace the quantum cloner in De Martini's experiment with a measure-and-prepare cloner. I explained in Section 2.2.3 that as there is a measurement in the measure-and-prepare amplification process, the entanglement between the two parties is broken and they are only classically correlated after the amplification process.

The next step is to consider the inaccuracy in measurements. Clearly the probability of getting each outcome is affected by getting other outcomes. That is because an outcome after some noise or loss, may be interpreted as a different outcome. For instance, consider the probability of detecting j photons in some basis when the state is $|\psi\rangle = \frac{|j-1\rangle + |j\rangle + |j+1\rangle}{\sqrt{3}}$. If the measurement is perfect, the probability of getting $|j\rangle$ is $\frac{1}{3}$. However if there is noise in the measurement, the $|j-1\rangle$ part of the state may be measured as $|j\rangle$. That changes the probability of getting $|j\rangle$. This change depends on the types of inaccuracy in measurements. To account for these inaccuracies, I coarse-grain the measurement outcomes. In this chapter, I stick to a simple coarse-graining method which is to average over neighbouring probabilities. Mathematically, that is

$$\bar{Pr}(j) = P(j) + P(j+1). \tag{3.1}$$

This is the most basic way of coarse-graining the measurement outcomes. Indeed, this is a non-overlapping binning with bins of size 2. I picked this model to show that even for small inaccuracies in measurement, there is a classical correlation which could approximate the micro-macro entanglement in De Martini's experiment. In the next chapter, I will replace this coarse-graining model with a more structured model with larger bins but in this chapter, this model serves my purpose.

There are two bipartite systems, one with classical correlation and one with quantum entanglement. First, I calculate the measurement outcomes for these two systems and coarse-grain the result. Then I compare the two sets of coarse-grained outcomes. The comparison in this chapter is an intuitive graphical comparison. I will quantify this comparison in the next chapter.

In this section, I will explain all these steps in more detail. I will start with a system with classical correlations. Then I will derive the probability distributions for the measurement outcomes for the two systems and finally I will compare the coarse-grained results.

3.2.1 Micro-Macro system with classical correlation

For the system with classical correlations, I consider a set-up similar to De Martini's experiment, but instead of sthe phase covariant cloner, I use a measure-and-prepare cloner as introduced in Section 2.2.3. This means the photon in channel B is being measured in some random basis on the equator and the cloner prepares N copies of the measurement outcome. The measurement of the single photon on channel B breaks the entanglement which means that the state after amplification is only classically correlated with the single photon on channel A.

This approach was introduced by P. Sekatski et al. in [14]. As I described the measure-and-prepare cloner in Section 2.2.3, the state of the amplified qubit is

$$\rho_{mp} = \frac{1}{\pi} \int d\phi_{mp} \left(P^{+}(\phi_{mp}) \mid \Phi_{\phi_{mp}} \rangle \langle \Phi_{\phi_{mp}} \mid + P^{-}(\phi_{mp}) \mid \Phi_{\phi_{mp}\perp} \rangle \langle \Phi_{\phi_{mp}\perp} \mid \right), \tag{3.2}$$

where the state $\mid \Phi_{\phi_{mp}} \rangle$ is

$$\mid \Phi_{\phi} \rangle = |N\rangle_{\phi} = \frac{\left(a_{\phi}^{\dagger}\right)^{N}}{\sqrt{N!}} |0\rangle. \tag{3.3}$$

As already discussed in Section 2.2.3, this cloner is optimal and in the limit $N \to \infty$, the fidelity of the clones is $\frac{3}{4}$. .

I refer to the classical system as *MP-cloner* and to De Martini's experiment as *PC-cloner.* Now the question is whether or not MP-cloner can approximate the statistics of PC-cloner.

3.2.2 Probability distributions

In this section I find the probability distributions for MP-cloner and PC-cloner. To compare, I study possible measurements on them and compare the probability distribution of outcomes. There are two measurements, one for the single photon on channel A and one for the beam of light on channel B. The measurement of the single photon is a single photon detection and determines the state of the photon in the measurement basis.The measurement on the multi-photon state counts the number of photons in two orthogonal mode of a given basis, e.g. j in the $|R\rangle$ state and $N - j$ photons in the $|L\rangle$ state.

As the initial state is a singlet state, measurement of the single photon determines the state of the photon on channel B before the amplification and consequently the final macro-state. For instance, suppose the measurement basis to be $\{|1,0\rangle_{\theta_A,\phi_A}, |0,1\rangle_{\theta_A,\phi_A}\}$. If the outcome of the single photon measurement is $|1,0\rangle_{\theta_A,\phi_A}$, then the state on channel B is $|0,1\rangle_{\theta_A,\phi_A}$. In other words, the measurement of the single photon in channel A determines the input state for the amplification process and introduces two new parameters,

θ_A and ϕ_A. I call these two parameters θ_{in} and ϕ_{in} as they specify the input state for the amplification process. For equatorial measurements, $\theta_{in} = \pi/2$ and there is only one parameter, ϕ_{in}. Therefore I drop the index for θ_{in} for simplicity and only keep ϕ_{in} in my notation.

As mentioned before, measurements on the macro-state are photon-counting measurements. In order to calculate the probability distribution for measurements on the macro-state, I calculate the macro state first. Macro qubit is different in between PC-cloner and MP-cloner.

Macro-state for PC-cloner

As explained in Section 2.2.3 the evolution in PC-cloner corresponds to the following Hamiltonian:

$$H = i\chi a_h^\dagger a_v^\dagger + H.c.. \tag{3.4}$$

Therefore the macro-state is:

$$|\psi_{PC}\rangle = e^{-itH}|\psi_{input}\rangle. \tag{3.5}$$

An arbitrary single-photon input state on the equator can be parametrized as:

$$|\ \psi_{input}\rangle = \cos(\phi)|1,0\rangle_{\frac{\pi}{2},0} + \sin(\phi)|0,1\rangle_{\frac{\pi}{2},0}. \tag{3.6}$$

Here I follow a similar method as in [13] to calculate the macro state. Rewriting the Hamiltonian in the form of Eq. [2.24], breaks the time evolution operator into two unitaries:

$$e^{-itH} = e^{\frac{g}{2}(a^{\dagger 2}-a^2)}e^{\frac{g}{2}(a_\perp^{\dagger\,2}-a_\perp^2)} = UU_\perp. \tag{3.7}$$

If one span the Hilbert space of the input photon in $\{|R\rangle = |1\rangle_0|0\rangle_{0\perp}, |L\rangle = |0\rangle_0|1\rangle_{0\perp}\}$ basis, the amplified basis is:

$$\begin{aligned}\{|\Phi^R\rangle =& UU_\perp|1,0\rangle_0 = |A_1\rangle|A_0\rangle_\perp,\\ |\Phi_\perp^L\rangle =& UU_\perp|0,1\rangle_0 = |A_0\rangle|A_1\rangle_\perp\},\end{aligned} \tag{3.8}$$

where $|A_1\rangle = U|1\rangle, |A_0\rangle = U|0\rangle$, and analogously for the perpendicular modes. The explicit form of $|\Phi^{\phi}_{B}\rangle$ and $|\Phi^{\phi\perp}_{B}\rangle$ for an arbitrary ϕ is:

$$|\Phi^{\phi}\rangle_B = \sum_{i,j=0}^{\infty} \gamma_{ij} \frac{\sqrt{(1+2i)!(2j)!}}{i!j!} \left|(2i+1)\phi; (2j)\phi^{\perp}\right\rangle_B \tag{3.9}$$

$$|\Phi^{\phi\perp}\rangle_B = \sum_{i,j=0}^{\infty} \gamma_{ij} \frac{\sqrt{(1+2i)!(2j)!}}{i!j!} \left|(2j)\phi; (2i+1)\phi^{\perp}\right\rangle_B, \tag{3.10}$$

with $\gamma_{ij} \equiv C^{-2}(-\frac{\Gamma}{2})^i \frac{\Gamma}{2}$, $C \equiv \cosh g$, $\Gamma \equiv \tanh g$, and g the non-linear gain. The two macro-states $|\Phi^{\phi}_{B}\rangle$ and $|\Phi^{\phi\perp}_{B}\rangle$ are orthogonal which indicates the state $|\Sigma\rangle$ in Eq. [2.31] is still a singlet state. For more detail see [4].

The time evolution operator is linear, which means that a general input state is a superposition of $|\Phi^{\phi}_{B}\rangle$ and $|\Phi^{\phi\perp}_{B}\rangle$ as:

$$|\psi_{PC}\rangle = e^{-itH}(\cos(\phi)|1,0\rangle_{\frac{\pi}{2},0} + \sin(\phi)|0,1\rangle_{\frac{\pi}{2},0}) = \cos(\phi)|\Phi^{\phi}_{B}\rangle + \sin(\phi)|\Phi^{\phi\perp}_{B}\rangle. \tag{3.11}$$

This is the macro-state that I study for measurements.

Macro-state for MP-cloner

As I am using the measure-and-prepare cloner for amplification in MP-cloner, the macro state as in Eq. [2.27] is:

$$\rho_{mp} = \frac{1}{\pi} \int d\phi_{mp} (P^{+}(\phi_{mp}) \mid \Phi_{\phi_{mp}}\rangle\langle\Phi_{\phi_{mp}} \mid + P^{-}(\phi_{mp}) \mid \Phi_{\phi_{mp}\perp}\rangle\langle\Phi_{\phi_{mp}\perp} \mid), \tag{3.12}$$

For an input state on the equator, the probabilities $P^{\pm}(\phi)$ are:

$$P^{+}(\phi) = \cos\left(\frac{\phi}{2}\right), \quad P^{-}(\phi) = \sin\left(\frac{\phi}{2}\right). \tag{3.13}$$

The parameter ϕ denotes the polar angle on the equator. see Figure [2.1] for more detail.

Measurements on macro-states and final probability distributions

Now that I have the macro-state for both PC-cloner and MP-cloner, I can apply projective measurements to them and calculate the probability distribution of outcomes.

The measurement on the macro-state involves a phase rotator, a polarizing beam splitter and two photon counting detectors. See Figure [2.2] for more detail. After the amplification, the phase rotator and the beam splitter separates photons into an arbitrary orthogonal polarizations basis e.g. $|\Phi_\phi\rangle, |\Phi_{\phi\perp}\rangle$. There are two photon detectors after the beam splitter. One of them counts the number of photons in the state $|\Phi_\phi\rangle$ and the other one those in the orthogonal state $|\Phi_{\phi\perp}\rangle$.

The polarization rotator determines the basis of measurement on the macro state and introduces two new parameters θ_{out} and ϕ_{out}. As the amplification process for both cloner is phase covariant, the parameter ϕ_{in} does not matter and I set it to zero without loss of generality. In fact, only the difference between ϕ_{in} and ϕ_{out} is relevant, so I merge them together to one parameter $\Delta\phi = \phi_{in} - \phi_{out}$ for this study. As I am still working with equatorial measurements in this chapter, I choose $\theta_{out} = \frac{\pi}{2}$.

The projection operator corresponding to this photon counting measurement is:

$$\Pi_j = |j, N-j\rangle\langle j, N-j|_{\frac{\pi}{2},\Delta\phi}.$$

Then the probability distribution for PC-cloner is:

$$Pr_{pc}(j,\, \Delta\phi) = \left\| \langle \Psi_{pc} | j, N-j\rangle_{\Delta\phi} \right\|^2. \tag{3.14}$$

Similarly the probability distribution for MP-cloner is:

$$Pr_{mp}(j,\, \Delta\phi) = \frac{1}{\pi}\int_0^\pi d\phi_{mp} P^{+}(\phi_{mp}) \left\| {}_{\phi_{mp}}\langle N | j, N- j\rangle_{\Delta\phi} \right\|^2. \tag{3.15}$$

For the explicit form of the probability distribution in Eq. [3.14,3.15] see [Appendix A].

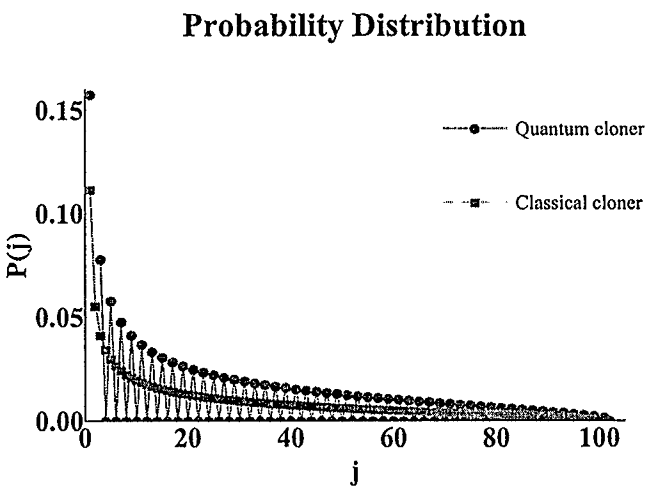

Figure 3.2: Probability distributions for classical and quantum mechanically amplified states for $\Delta\phi = 0$. The x-axis indicates possible out comes on detector B1 as in Figure [2.2] and the y-axis the probability of getting that outcome.

3.3 Results

Here I compare PC-cloner with MP-cloner. I will quantify this comparison in the next chapter.

Figure [3.2] shows the probability distribution for the two macro-states when $\Delta\phi = 0$.

For perfect measurements, it is possible to distinguish these two macro-states, as the macro-state for PC-cloner has zero probability for even terms, while MP-cloner has non-zero probabilities.

On the other hand, from a realistic viewpoint, as measurement are not perfect, the probability distribution in a real experiment would be coarse-grained. As I explained in Section 3.2, for coarse-graining I start with the simple non-overlapping binning of Eq. [3.1]. That is:

$$\bar{Pr}(j) = P(j) + P(j+1). \tag{3.16}$$

Figure [3.3] shows the coarse-grained version of Figure [3.2]. If photon counting

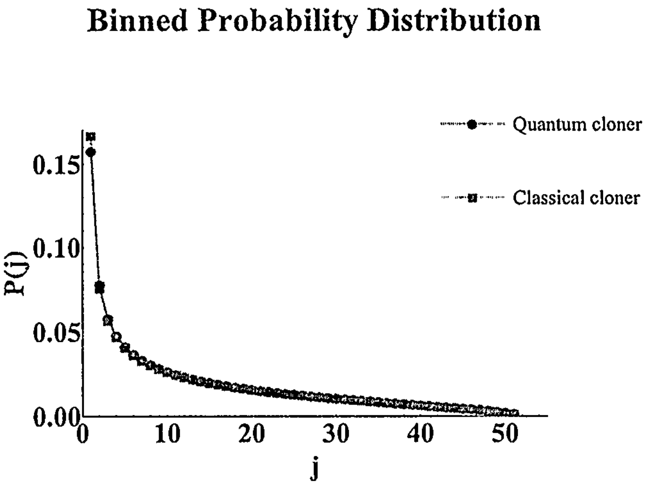

Figure 3.3: Coarse-Grained probability distributions. The x-axis indicates possible outcomes after coarse-graining and the y-axis indicates the probability of getting coarse-grained outcomes.

detectors cannot resolve neighbouring terms, i.e. $|j, N-j\rangle$ from $|j+1, N-j-1\rangle$, then the final probability distribution looks like Figure [3.3].

Clearly, for even the most basic coarse-graining model that I considered here, the quantum entanglement in De Martini's experiment is not easily distinguishable from the classical correlation in my separable micro-macro proposal. This is the core idea of my work, that when measurement outcomes are coarse-grained, the quantum correlation can be well approximated classically. Note that I took $\Delta\phi = 0$ but the result here holds for any arbitrary $\Delta\phi$. For more detail, see Section A.3.

3.4 Summary

For the demonstration of entanglement that De Martini et al. presented in [4], even small inaccuracies in measurements make it almost impossible to distinguish quantum entanglement from classical correlations. In other words, if measurements are not perfect, the statistics of De Martini's experiment can be approximated with a classically correlated system. This is an example that illustrates that coarse-graining can result in the emergence of classical physics from quantum effects.

In the next chapter, I will extend my study to general measurements on Bloch sphere for both the single photon and the beam of light. There I will generalize the two parameters θ_{in} and θ_{out}. I will modify the measure-and-prepare cloner in the classical micro-macro proposal for comparison with general measurements. I will also present a more general model for coarse-graining the measurement outcomes. Finally, I will quantify the difference between measurements on PC-cloner and the new MP-cloner. This will lead me to conclude that it is difficult to observe the micro-macro entanglement in De Martini's experiment when measurements are not exact, which is the central message of this thesis.

Chapter 4

Micro-Macro Entanglement Under General Coarse-grained Measurements

In Chapter 3, I considered De Martini's experiment with their equatorial measurements. The question I will be considering within this chapter is whether or not there is any basis for photon counting measurement that distinguishes the micro-macro entanglement from a classical correlation.

I follow a similar method as in Chapter 3. Concerning the proposals, there are 2 changes. First, measurements for both PC-cloner and MP-cloner is now extended to measurements in an arbitrary basis on Bloch sphere. This generalizes the two parameters θ_{in} and θ_{out} and changes the action of polarization rotators. The second change concerns the MP-cloner only. As I will explain in Section 4.1.1, the primary measure-and-prepare cloner should be modified to fit generalized measurements.

There are also some changes in mathematical details of coarse-graining and the comparison between two proposals. Here I will present a more general model for coarse-graining. I also quantify the concept of comparison with a statistical distance. Finally I will show that the statistical distance between PC-cloner and MP-cloner goes to zero as the precision of measurements decreases.

The structure of this chapter is as follows: in the first section, I will explain why MP-cloner I used in Chapter 3 is not good enough for measurements in all bases. Then in Section 4.1.2 I will calculate the probability distribution for measurements in an arbitrary basis. Finally in Section 4.2 I will compare the new class of MP-cloner with PC-cloner for measurements in an arbitrary basis and present my results.

4.1 Method

The method is similar to what I did in the previous chapter. Here I will go through what is different. In the first part of this section, I will explain why the primary MP-cloner proposal does not fit for general measurement and propose a new MP-cloner. The rest is to calculate the probability distribution and to compare them. In Section 4.1.3 I will present the new structured coarse-graining model and finally in Section 4.1.4 I introduce a mathematical measure to quantify the difference between PC-cloner and MP-cloner.

4.1.1 New measure-and-prepare cloner

Although the measure-and-prepare cloner I exploited in previous chapter works very well when measurements are equatorial, measurements on the pole of Bloch spherewould differentiate it from PC-cloner. That is because the state amplified with the phase covariant cloner is highly squeezed for measurements in J_z, introduced in Eq. [2.3]. To see that, consider the amplification Hamiltonian in Eq. [2.23]:

$$H = i\chi(\left(a_{\phi}^{\dagger}\right)^2 + \left(a_{\phi\perp}^{\dagger}\right)^2) + H.c.,$$

Clearly it generates the same number of photons in both $|H\rangle$ and $|V\rangle$ polarizations and the difference between the number of photons in $|H\rangle$ and $|V\rangle$ for the input state is close to one. When the cloner amplifies it to $N \approx 10^4$ photons, the difference is still 1 which means that the state is highly squeezed.

On the other hand, the primary measure-and-prepare cloner involves production of $|N\rangle_{\phi}$ on the equator. One can expand the state in the $|H\rangle$ and $|V\rangle$ basis. In that basis, the state has terms like $|10^4, 0\rangle_{h,v}$ which is not squeezed at all.

That means to differentiate the two cloners, one can simply do measurements on the pole of Bloch sphere namely in $\{|H\rangle, |V\rangle\}$. Note that this difference could not be demonstrated by equatorial measurements.

The tricky point here is that, although my primary MP-cloner is distinguishable from PC-cloner , it still does not mean that correlation in PC-cloner could not be approximated classically. In other words, one may still find an other classical system that works better and it could approximate the correlation of PC-cloner for measurements in an arbitrary basis. That is what I will cover in this section.

I propose a new MP-cloner which is to approximate PC-cloner for photon counting measurements in any arbitrary basis. Based on the problem I mentioned above, a natural choice is to confine the measure-and-prepare cloner to generate squeezed states, states with small ΔJ_z. That means instead of $|N\rangle_\phi = \sum_i c_i(\phi)|i,\, N-i\rangle_{h,v}$ I only keep squeezed terms of the decomposition which in the extreme case is:

$$|\Phi_\phi\rangle = \frac{e^{i\phi}|n,\, n+1\rangle + e^{-i\phi}|n+1,\, n\rangle}{\sqrt{2}}, \tag{4.1}$$

where $n = \frac{N-1}{2}$. This state is highly squeezed but it has the problem that equatorial measurements distinguishes it from PC-cloner. Therefore, as a compromise, I can keep more terms which are less squeezed but this improves MP-cloner for equatorial measurements. I take the following state for MP-cloner:

$$|\Phi_\phi\rangle = \frac{1}{\sqrt{2(t+1)}}\sum_{j=0}^{t}(e^{i\phi(2i+1)}|n-i,\, n+i+1\rangle + e^{-i\phi(2i+1)}|n+i+1,\, n-i\rangle), \tag{4.2}$$

where t indicates how many less squeezed terms I am keeping. In fact $t = 0$ is the most squeezed case and as t increases, the state becomes less squeezed. This introduces a new parameter, t.

4.1.2 Probability distribution for measurements in an arbitrary basis

The next step is to calculate the probability distribution corresponding to measurement outcomes. I follow the exact same procedure as I did in Section 3.2.2 with a different state and different measurements. The probability for MP-cloner is:

$$Pr_{mp}(j,\, \theta_{out},\, \theta_{in},\, \Delta\phi) = \frac{1}{\pi}\int_0^{\pi} d\phi_{mp} P^{+}(\phi_{mp}, \theta_{in}) \left\| \langle \Phi_{\phi_{mp}} | j, N-j\rangle_{\theta_{out},\Delta\phi} \right\|^2 . \tag{4.3}$$

Clearly more parameters are involved in this probability distribution. That is because θ_{out}, $\theta_{in} \neq \pi/2$ any more.

Similarly, the probability distribution for the measurement in an arbitrary basis on macro-state of PC-cloner would change to:

$$Pr_{pc}(j,\, \theta_{out},\, \theta_{in},\, \Delta\phi) = \left\| \langle \Psi_{pc}(\theta_{in}) | j, N-j \rangle_{\theta_{out},\Delta\phi} \right\|^2 . \tag{4.4}$$

For the explicit form of probability distribution see [Appendix B].

4.1.3 Coarse-graining Model

The next step is to specify the coarse-graining method. I model the coarse-graining as a symmetric overlapping binning with the following form:

$$\bar{Pr}(j) = \frac{Pr(j-\sigma) + \ldots + Pr(j) + \ldots + Pr(j+\sigma)}{2\sigma+1}, \tag{4.5}$$

where the size of the bin is $2\sigma + 1$. The parameter σ should be determined by the amount of error that there exists in outcomes, i.e. if there is too much error that means the inaccuracy in outcomes is large and each probability is affected by a larger bin, therefore σ should be larger.

I have tried several different approaches for modelling coarse-graining and I strongly expect that the results do not depend on the coarse-graining method.

4.1.4 Measure for comparison

In order to quantify the distance between the two types of correlation, I use the Manhattan norm which is defined as:

$$D = \sum_j |Pr_{pc}(j) - Pr_{mp}(j)| . \tag{4.6}$$

This is a global measure of statistical difference between the two probability distributions. For more information see [37].

4.2 Results

The result of this section is summarized in Figure [4.1]. It shows how the difference changes as a function of the relative bin size, σ/N. As expected, the more coarse-graining, the less distant they become. This implies that it would be more difficult to distinguish the micro-macro entanglement from classical correlations.

For larger coarse-graining the distance become smaller and smaller. Note that D is a function of all angles, as was discussed before. This means, one should make sure that this behaviours hold for all different values of parameters. I did the same graph for different values of parameters and results are similar. See [Appendix B] for more details.

There still might be a caveat here. In my simulation, the largest value of N is 91 which is fairly small in comparison to $N \simeq 10^4$ in the experiment. One might object that although the difference between classical and quantum mechanical result is small after coarse-graining for small values of N, this could be false when N is large. Figure [4.1] fills this caveat. This graphs shows that as the parameter N increases, not only the difference has the same behaviour, but it also decreases faster in terms of the relative error, $\frac{\sigma}{N}$.

This means that for the real experiment which has $N \simeq 10^4$, for a very small inaccuracy, the distance between classical and quantum mechanical outcome vanishes.

Figure [4.2] gives a clear picture for larger values of σ. When σ grows, the distance becomes almost independent of N. On the other hand, for large values of N , the same σ corresponds to a smaller relative error. In other words, large σ guarantees that distance is small and does not depend on N. Therefore, for relatively small errors, the two types of correlations become indistinguishable.

Figure [4.2] and Figure [4.1] are for $\theta_{in} = \frac{\pi}{2}, \theta_{out} = \frac{\pi}{12}, \Delta\phi = 0$. I found similar graphs for other values of parameters. See [Appendix B]

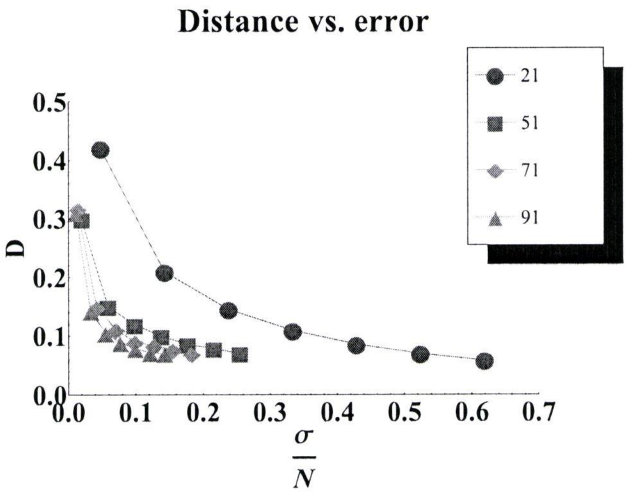

Figure 4.1: This graphs shows $D(j)$ as a function of the relative error $\frac{sigma}{N}$, for different value of N. As N increases, e.g. for $N \simeq 10^4$ the distance is expected to vanishes for even small inaccuracies.

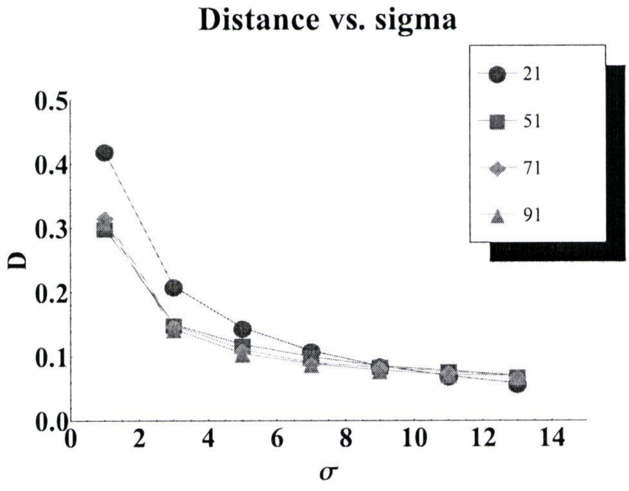

Figure 4.2: This graphs shows $D(j)$ as a function of $2\sigma + 1$, the size of the bin, for different value of N. For large values of the bin size, the distance for different values of N decreases to the same value.

4.3 Summary

I showed that the statistical difference between De Martini's experiment and my separable micro-macro proposal becomes negligible for even small amount of inaccuracy in photon counting measurements. Furthermore I showed that this result holds for photon counting measurements in any arbitrary basis. This demonstrates why it is difficult to observe the micro-macro entanglement in De Martini's experiment.

Chapter 5

Discussion and Conclusion

In this thesis, I studied De Martini's experiment for generating entanglement between a macroscopic and a microscopic object. I proposed a system with a purely classical correlation and I showed that if measurement outcomes are coarse-grained, statistical properties of De Martini's experiment looks like statistical properties of my classical proposal. This is a Quantum-to-Classical transition from the micro-macro entanglement to classical correlation that occurs only due to the coarse-graining of measurement outcomes.

Note that this is not in contrast to decoherence program as one still needs coherent evolution to see quantum effects. In other words, not only a coherent evolution is required to see quantum phenomena, but also precise measurements are needed. My result states that even if the evolution is perfectly coherent but measurements are not accurate, quantum entanglement vanishes and appears as a classical correlation.

I would like to mention that this is not the first time that Quantum-to-Classical transition under coarse-grained measurements has been studied. This approach was previously exploited in [8] to show a Quantum-to-Classical transition for spin systems. In that paper, Kofler et al. showed that the time evolution of a spin particles looks exactly like a classical spin if measurements of S_z operator are coarse-grained. The required resolution in order to distinguish non-classicality should be $\Delta m \lesssim \sqrt{j}$ where j is the total angular momentum of the spin system. A similar result was reported before in [38]. It states that for a specific class of states, all Bell inequalities will be satisfied if:

$$\Delta m \gg \sqrt{j}. \tag{5.1}$$

Here I showed that for the specific case of De Martini's experiment, a resolution of

$\Delta m \approx 1$ is required to see the non-classicality. This suggests that for some states, a higher resolution is required to demonstrate the non-classicality.

What I proved here is limited to De Martini's experiment and it does not mean that any micro-macro entanglement could be approximated with classical correlation after coarse-graining. In other words, although I proved that Schrödinger's cat that De Martini proposed is difficult to demonstrate, there might still exist a micro-macro entanglement that has no classical analogue and could be demonstrated. Therefore, a natural way to extend upon my work is to study other proposals for generating micro-macro entanglement e.g. opto-mechanical qubits[2]. The long-term goal would be to either prove that any micro-macro entanglement transits to classical correlation under the restriction of coarse-grained measurements or to find a feasible micro-macro entanglement that could not be approximated classically after coarse-graining.

Another direction to build up on my project is to find the maximum sufficient resolution to see non-classicality. This may depend on the state under study. Then it would be interesting to understand what properties of the state affect the sufficient resolution and how they affect it.

Bibliography

[1] J. R. Friedman, V. Patel, W. Chen, S. K. Tolpygo, and J. E. Lukens, "Quantum superposition of distinct macroscopic states," *Nature*, vol. 406, pp. 43–46, Jun 2000.

[2] J. D. Teufel, T. Donner, D. Li, J. W. Harlow, M. S. Allman, K. Cicak, A. J. Sirois, J. D. Whittaker, K. W. Lehnert, and R. W. Simmonds, "Sideband cooling of micromechanical motion to the quantum ground state," *Nature*, vol. 475, pp. 359–363, Jul 2011.

[3] A. D. OConnell, M. Hofheinz, M. Ansmann, R. C. Bialczak, M. Lenander, E. Lucero, M. Neeley, D. Sank, H. Wang, M. Weides, J. Wenner, J. M. Martinis, and A. N. Cleland, "Quantum ground state and single-phonon control of a mechanical resonator," *Nature*, vol. 464, pp. 697–703, Mar 2010.

[4] F. De Martini, F. Sciarrino, and C. Vitelli, "Entanglement test on a microscopic-macroscopic system," *Phys. Rev. Lett.*, vol. 100, p. 253601, Jun 2008.

[5] E. Schrödinger, "Die gegenwärtige Situation in der Quantenmechanik," *Naturwissenschaften*, vol. 23, pp. 807–812, Nov. 1935.

[6] W. H. Zurek, "Decoherence, einselection, and the quantum origins of the classical," *Rev. Mod. Phys.*, vol. 75, pp. 715–775, May 2003.

[7] W. H. Zurek, "Decoherence and the transition from quantum to classical," *Physics Today*, vol. 44, no. 10, pp. 36–44, 1991.

[8] J. Kofler and i. c. v. Brukner, "Classical world arising out of quantum physics under the restriction of coarse-grained measurements," *Phys. Rev. Lett.*, vol. 99, p. 180403, Nov 2007.

[9] A. Einstein, B. Podolsky, and N. Rosen, "Can quantum-mechanical description of physical reality be considered complete?," *Phys. Rev.*, vol. 47, pp. 777–780, May 1935.

[10] R. F. Werner, "Quantum states with einstein-podolsky-rosen correlations admitting a hidden-variable model," *Phys. Rev. A*, vol. 40, pp. 4277–4281, Oct 1989.

[11] A. Peres, "Collective tests for quantum nonlocality," *Phys. Rev. A*, vol. 54, pp. 2685–2689, Oct 1996.

[12] C. Simon and D. Bouwmeester, "Theory of an entanglement laser," *Phys. Rev. Lett.*, vol. 91, p. 053601, Aug 2003.

[13] P. Sekatski, N. Brunner, C. Branciard, N. Gisin, and C. Simon, "Towards quantum experiments with human eyes as detectors based on cloning via stimulated emission," *Phys. Rev. Lett.*, vol. 103, p. 113601, Sep 2009.

[14] P. Sekatski, B. Sanguinetti, E. Pomarico, N. Gisin, and C. Simon, "Cloning entangled photons to scales one can see," *Phys. Rev. A*, vol. 82, p. 053814, Nov 2010.

[15] H. S. Eisenberg, G. Khoury, G. A. Durkin, C. Simon, and D. Bouwmeester, "Quantum entanglement of a large number of photons," *Phys. Rev. Lett.*, vol. 93, p. 193901, Nov 2004.

[16] N. Spagnolo, C. Vitelli, F. Sciarrino, and F. De Martini, "Entanglement criteria for microscopic-macroscopic systems," *Phys. Rev. A*, vol. 82, p. 052101, Nov 2010.

[17] N. Herbert, "FLASH - A SUPERLUMINAL COMMUNICATOR BASED UPTON A NEW KIND OF QUANTUM MEASUREMENT," *Found. Phys.*, vol. 12, pp. 1171–1179, 1982.

[18] G. C. Ghirardi, T. Weber, and A. Rimini, "A GENERAL ARGUMENT AGAINST SUPERLUMINAL TRANSMISSION THROUGH THE QUANTUM MECHANICAL MEASUREMENT PROCESS," *Lett. Nuovo Cim.*, vol. 27, pp. 293–298, 1980.

[19] W. K. Wootters and W. H. Zurek, "A single quantum cannot be cloned," *Nature*, vol. 299, pp. 802–803, Oct 1982.

[20] L. MANDEL, "Is a photon amplifier always polarization dependent?," *Nature*, vol. 304, p. 188, Jul 1983.

[21] P. W. Milonni and M. L. Hardies, "Photons cannot always be replicated," *Physics Letters A*, vol. 92, no. 7, pp. 321 – 322, 1982.

[22] V. Bužek and M. Hillery, "Quantum copying: Beyond the no-cloning theorem," *Phys. Rev. A*, vol. 54, pp. 1844–1852, Sep 1996.

[23] D. Bruss, A. Ekert, and C. Macchiavello, "Optimal universal quantum cloning and state estimation," *Phys. Rev. Lett.*, vol. 81, pp. 2598–2601, Sep 1998.

[24] M. A. Nielsen and I. L. Chuang, *Quantum Computation and Quantum Information.* Cambridge University Press, 2000.

[25] N. Gisin and S. Massar, "Optimal quantum cloning machines," *Phys. Rev. Lett.*, vol. 79, pp. 2153–2156, Sep 1997.

[26] C. Simon, G. Weihs, and A. Zeilinger, "Optimal quantum cloning via stimulated emission," *Phys. Rev. Lett.*, vol. 84, pp. 2993–2996, Mar 2000.

[27] D. Bruß, M. Cinchetti, G. Mauro D'Ariano, and C. Macchiavello, "Phase-covariant quantum cloning," *Phys. Rev. A*, vol. 62, p. 012302, Jun 2000.

[28] F. Sciarrino and F. De Martini, "Realization of the optimal phase-covariant quantum cloning machine," *Phys. Rev. A*, vol. 72, p. 062313, Dec 2005.

[29] E. Nagali, T. De Angelis, F. Sciarrino, and F. De Martini, "Experimental realization of macroscopic coherence by phase-covariant cloning of a single photon," *Phys. Rev. A*, vol. 76, p. 042126, Oct 2007.

[30] A. J. Leggett and A. Garg, "Quantum mechanics versus macroscopic realism: Is the flux there when nobody looks?," *Phys. Rev. Lett.*, vol. 54, pp. 857–860, Mar 1985.

[31] M. Caminati, F. De Martini, R. Perris, F. Sciarrino, and V. Secondi, "Nonseparable werner states in spontaneous parametric down-conversion," *Phys. Rev. A*, vol. 73, p. 032312, Mar 2006.

[32] C. H. Bennett, D. P. DiVincenzo, J. A. Smolin, and W. K. Wootters, "Mixed-state entanglement and quantum error correction," *Phys. Rev. A*, vol. 54, pp. 3824–3851, Nov 1996.

[33] "Quantum computation, entanglement and state reduction," *Philosophical Transactions of the Royal Society of London. Series A: Mathematical, Physical and Engineering Sciences*, vol. 356, no. 1743, pp. 1927–1939, 1998.

[34] G. C. Ghirardi, A. Rimini, and T. Weber, "Unified dynamics for microscopic and macroscopic systems," *Phys. Rev. D*, vol. 34, pp. 470–491, Jul 1986.

[35] J. Kofler and C. Brukner, "Are there fundamental limits for observing quantum phenomena from within quantum theory?," 2010.

[36] A. J. Leggett, "Testing the limits of quantum mechanics: motivation, state of play, prospects," *Journal of Physics: Condensed Matter*, vol. 14, no. 15, p. R415, 2002.

[37] E. Krause, *Taxicab geometry: an adventure in non-Euclidean geometry.* Dover Publications, 1986.

[38] A. Peres, *Quantum theory: concepts and methods.* Fundamental theories of physics, Kluwer Academic Publishers, 1995.

Appendix A

Equatorial probability distributions

In this Appendix, I present the explicit form of the probability distribution for equatorial measurements for PC-cloner and MP-cloner. I will also that as in Figure [3.3], for all values of parameter $\Delta\phi$, the probability distribution for both classical and quantum correlation look the same after coarse-graining. In part A I present the probability distribution for PC-cloner, and in part B the probability distribution for MP-cloner.

A.1 Probability distribution for PC-cloner

I will start with the $\Delta\phi = 0$ and π. Explicit probability distributions for these two cases are:

$$\begin{aligned} Pr_{\mathrm{pc}}(j,0) &= \frac{j!(n-j)!}{\left(\frac{j}{2}!\frac{n-j-1}{2}!\right)^2} \\ Pr_{\mathrm{pc}}(j,\pi) &= \frac{t!(n-j)!}{\left(\frac{j-1}{2}!\frac{n-j}{2}!\right)^2}, \end{aligned} \tag{A.1}$$

where $n = \frac{N-1}{2}$. The general probability distribution in terms $Pr_{\mathrm{pc}}(j,0)$ and $Pr_{\mathrm{pc}}(j,\pi)$ is:

$$\begin{aligned} Pr_{\mathrm{pc}}(j,\Delta\phi) =& \mathrm{Cos}^2(\frac{\Delta\phi}{2})Pr_{\mathrm{pc}}(j,0) + \mathrm{Sin}^2(\frac{\Delta\phi}{2})Pr_{\mathrm{pc}}(j,\pi) \\ &+2\mathrm{Sin}(\frac{\Delta\phi}{2})\mathrm{Cos}(\frac{\Delta\phi}{2})\sqrt{Pr_{\mathrm{pc}}(j,0)Pr_{\mathrm{pc}}(j,\pi)} \end{aligned} \tag{A.2}$$

A.2 Probability distribution for PC-cloner

It is similar to the previous section. I start with the $Pr_{\text{mp}}(j,0)$ and $Pr_{\text{mp}}(j,0)$ which are:

$$\begin{aligned} Pr_{\text{mp}}(j,0) &= \frac{2*n!}{\pi(n-j)!j!}\text{Beta}\left(j+1/2, n-j+3/2\right) \\ Pr_{\text{mp}}(j,\pi) &= \frac{2*n!}{\pi(n-j)!j!}\text{Beta}\left(j+3/2, n-j+1/2\right), \end{aligned} \tag{A.3}$$

where $\text{Beta}(a,b) = \frac{\Gamma(a)\Gamma(b)}{\Gamma(a+b)}$ gives the Euler beta function. Then the general probability distribution is:

$$\begin{aligned} Pr_{\text{mp}}(j,\Delta\phi) =& \text{Cos}^2(\frac{\Delta\phi}{2})Pr_{\text{mp}}(j,0) + \text{Sin}^2(\frac{\Delta\phi}{2})Pr_{\text{mp}}(j,\pi) \\ &+2\text{Sin}(\frac{\Delta\phi}{2})\text{Cos}(\frac{\Delta\phi}{2})\sqrt{Pr_{\text{mp}}(j,0)Pr_{\text{mp}}(j,\pi)} \end{aligned} \tag{A.4}$$

Both $Pr_{\text{pc}}(j,\Delta\phi)$ and $Pr_{\text{mp}}(j,\Delta\phi)$ are the same functions of $Pr(j,\Delta\phi = 0)$ and $Pr_{\text{mp}}(j,\Delta\phi = \pi)$. Therefore, showing that under coarse-grained photon counting measurements, $\{Pr_{\text{pc}}(j,0), Pr_{\text{pc}}(j,\pi)\}$ looks like $\{Pr_{\text{mp}}(j,0), Pr_{\text{mp}}(j,\pi)\}$, is sufficient to prove that for any $\Delta\phi$, after coarse-graining the two probability distributions look the same.

A.3 Measurements with non-zero $\Delta\phi$

In Figure [3.3], I showed that for equatorial measurements with $\Delta\phi = 0$, if the photon counting outcomes are coarse-grained, the two graphs match each other. Figure [A.1] shows the same result for $\Delta\phi = \pi$. As I explained above, this figure extends my statement to any arbitrary $\Delta\phi$.

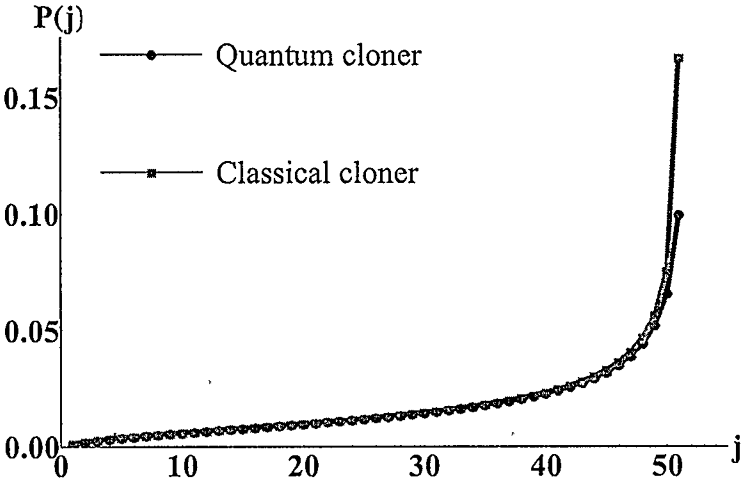

Figure A.1: Coarse-grained probability distribution for $\Delta\phi = \pi$ with equatorial measurements

Appendix B

General probability distributions

In this Appendix, I present the explicit form of the probability distribution for general measurements for PC-cloner and MP-cloner. I will also show that for all angles the statistical distance between PC-cloner and MP-clonervanishes. In part A I present the probability distribution for PC-cloner and in part B the probability distribution for MP-cloner.

B.1 Probability distribution for PC-cloner

I first define following functions:

$$\begin{aligned}
\mathrm{fp}\left(\theta \mathrm{in}, \Delta\phi\right) &= \frac{\mathrm{Cos}\left(\frac{\theta_{in}}{2}\right) e^{i*\Delta\phi} + \mathrm{Sin}\left(\theta_{in}/2\right) e^{-i*\Delta\phi}}{\sqrt{2}}, \\
\mathrm{cfp}\left(\theta_{in}, \Delta\phi\right) &= \frac{\mathrm{Cos}\left(\frac{\theta_{in}}{2}\right) e^{-i*\Delta\phi} + \mathrm{Sin}\left(\frac{\theta_{in}}{2}\right) e^{i*\Delta\phi}}{\sqrt{2}}, \\
\mathrm{fm}\left(\theta_{in}, \Delta\phi\right) &= -i\frac{\mathrm{Cos}\left(\frac{\theta_{in}}{2}\right) e^{i*\Delta\phi} - \mathrm{Sin}\left(\frac{\theta_{in}}{2}\right) e^{-i*\Delta\phi}}{\sqrt{2}}, \\
\mathrm{cfm}\left(\theta_{in}, \Delta\phi\right) &= i\frac{\mathrm{Cos}\left(\frac{\theta_{in}}{2}\right) e^{-i*\Delta\phi} - \mathrm{Sin}\left(\frac{\theta_{in}}{2}\right) e^{+i*\Delta\phi}}{\sqrt{2}}.
\end{aligned} \tag{B.1}$$

$$\begin{aligned}
&A\left(\mathrm{j}, \theta \text{ out}, \theta_{in}, \Delta\phi\right) = \sqrt{j!(2n+1-j)!}\,\mathrm{Cos}\left(\frac{\theta_{out}}{2} - \frac{\pi}{4}\right)^{2n+1-j} * \mathrm{Sin}\left(\frac{\theta_{out}}{2} - \frac{\pi}{4}\right)^{j} \\
&\sum_{p_1=0}^{j} \sum_{p_2=0}^{2*n+1-j} \Bigg(\frac{(p_1+p_2)!(2*n+1-p_1-p_2)!}{(j-p_1)!p_1!(2n+1-j-p_2)!p_2!} \mathrm{Cos}\left(\frac{\theta \mathrm{out}}{2} - \frac{\pi}{4}\right)^{p_1-p_2} * \mathrm{Sin}\left(\frac{\theta \mathrm{out}}{2} - \frac{\pi}{4}\right)^{p_2-p_1} \\
&*(-i)^{p_2-p_1} * \left(\frac{\mathrm{fp}\left(\theta_{in}, \Delta\phi\right) * \delta_{1,\mathrm{Mod}(p_1+p_2,2)}}{\left(\frac{p_1+p_2-1}{2}\right)!\left(\frac{2n+1-p_1-p_2}{2}\right)!} + \frac{\mathrm{fm}\left(\theta \mathrm{in}, \Delta\phi\right) * \delta_{0,\mathrm{Mod}(p_1+p_2,2)}}{\left(\frac{p_1+p_2}{2}\right)!\left(\frac{2n-p_1-p_2}{2}\right)!} \right)\Bigg).
\end{aligned} \tag{B.2}$$

Then the probability distribution is:

$$Pr_{\mathrm{pc}}(\mathrm{j}, \theta\ \mathrm{out}, \theta_{in}, \Delta\phi) = \mid A(\mathrm{j}, \theta\ \mathrm{out}, \theta_{in}, \Delta\phi) \mid^2 . \tag{B.3}$$

B.2 Probability distribution for MP-cloner

Similarly, I first define two following functions:

$$\begin{aligned}
mpA(j, t, \theta_{out}) &= \mathrm{Re}\Bigg(\sqrt{(2n{+}1{-}j)!j!(n-s)!(n+s+1)!}(-1)^{n-s} \\
&\sum_{p_1=\mathrm{Max}(0,j-n-s-1)}^{\mathrm{Min}(j,n-s)} \frac{(-1)^{p_1}}{(j-p_1)!p_1!} \frac{\mathrm{Cos}\left(\frac{\theta_{out}}{2}\right)^{2p_1+n-j+s+1} \mathrm{Sin}\left(\frac{\theta_{out}}{2}\right)^{n-s+j-2p_1}}{(n+s-j+p_1+1)!(n-s-p_1)!}\Bigg), \\
mpB(j, t, \theta_{out}) &= \mathrm{Re}\Bigg(\sqrt{(2n{+}1{-}j)!j!(n-s)!(n+s+1)!}(-1)^{n+s+1} \\
&\sum_{p_1=\mathrm{Max}(0,j+s-n)}^{\mathrm{Min}(j,n+s+1)} \frac{(-1)^{p_1}}{(j-p_1)!p_1!} \frac{\mathrm{Cos}\left(\frac{\theta_{out}}{2}\right)^{2p_1+n-j-s} \mathrm{Sin}\left(\frac{\theta_{out}}{2}\right)^{n+s+1+j-2p_1}}{(n-s-j+p_1)!(n+s+1-p_1)!}\Bigg)
\end{aligned} \tag{B.4}$$

Then the probability distribution is:

$$\begin{aligned}
&Pr_{\mathrm{mp}}(j, s, \theta_{out}, \theta_{in}, \Delta\phi) = \\
&\frac{1}{2(ts+1)}\Bigg(\sum_{\mathrm{i1}=0}^{ts}\sum_{\mathrm{i2}=0}^{ts}\Bigg(\frac{e^{2i*\Delta\phi(\mathrm{i1}-\mathrm{i2})}}{2} mpA(j, \mathrm{i1}, \theta_{out})\, mpA(j, \mathrm{i2}, \theta_{out}) \\
&(\mathrm{Cos}(2\alpha)(\delta_{\mathrm{i1},\mathrm{i2}+1} + \delta_{\mathrm{i1},\mathrm{i2}-1}) + 2\delta_{\mathrm{i1},\mathrm{i2}}) + \\
&\frac{e^{-2i*\Delta\phi(\mathrm{i1}-\mathrm{i2})}}{2} mpB(j, \mathrm{i1}, \theta_{out})\, mpB(j, \mathrm{i2}, \theta_{out}) \\
&(\mathrm{Cos}(2\alpha)(\delta_{\mathrm{i1},\mathrm{i2}+1} + \delta_{\mathrm{i1},\mathrm{i2}-1}) + 2\delta_{\mathrm{i1},\mathrm{i2}})) + \\
&\mathrm{Cos}(2\alpha)\,\mathrm{Cos}(2\Delta\phi)\, mpA(j, 0, \theta_{out})\, mpB(j, 0, \theta_{out}))
\end{aligned} \tag{B.5}$$

where $\alpha = \frac{\theta_{in}}{2} - \frac{\pi}{4}$

B.3 Graphs for general measurements

This section is to show that the result of Section 4.2 holds for all different values of parameters. Table B.1 shows how the difference between PC-cloner and MP-cloner changes for different values of parameters, θ_{out}, θ_{in}, $\Delta\phi$

Table B.1: Statistical distance between PC-cloner and MP-cloner as a function of error and bin size for different angles.

Distance vs. relative error	Distance vs. the size of the bin
θout=$\frac{\pi}{12}$, θin=$\frac{\pi}{12}$, $\Delta\phi$=0 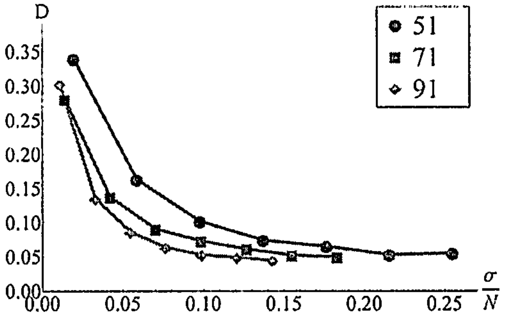	θout=$\frac{\pi}{12}$, θin=$\frac{\pi}{12}$, $\Delta\phi$=0 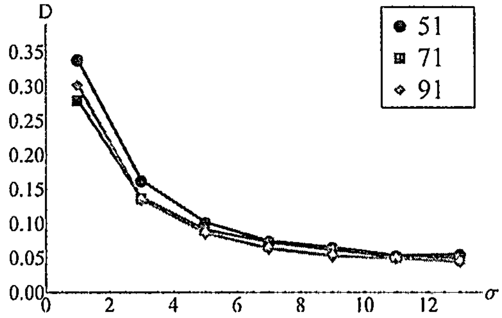
θout=$\frac{\pi}{12}$,θin=$\frac{\pi}{4}$,$\Delta\phi$=0 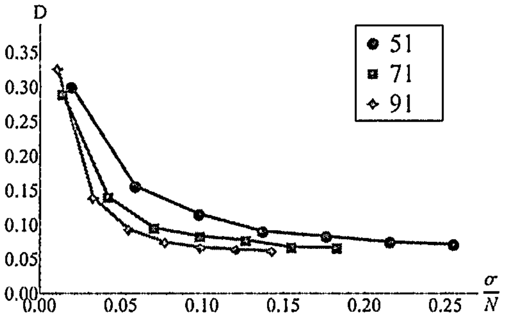	θout=$\frac{\pi}{12}$, θin=$\frac{\pi}{4}$, $\Delta\phi$=0 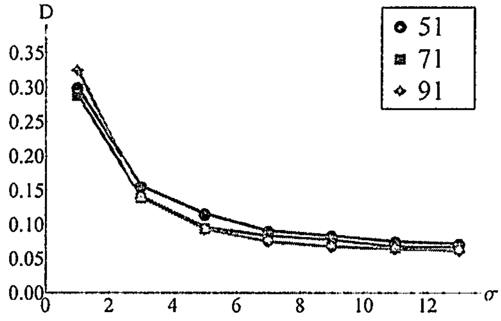

Continued on Next Page...

Table B.1 – Continued

Distance vs. relative error	Distance vs. the size of the bin
$\theta\text{out}=\frac{\pi}{12},\theta\text{in}=\frac{5\pi}{12},\Delta\phi=0$ 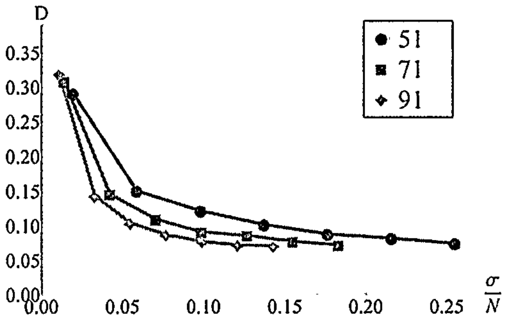 	$\theta\text{out}=\frac{\pi}{12},\ \theta\text{in}=\frac{5\pi}{12},\ \Delta\phi=0$ 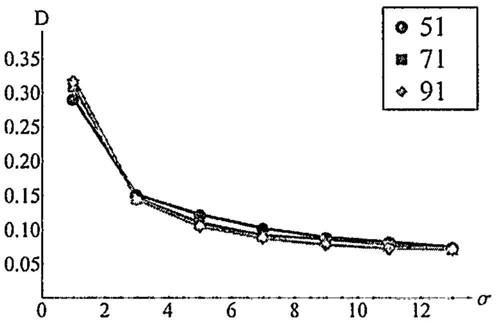
$\theta\text{out}=\frac{\pi}{4},\theta\text{in}=\frac{\pi}{4},\Delta\phi=0$ 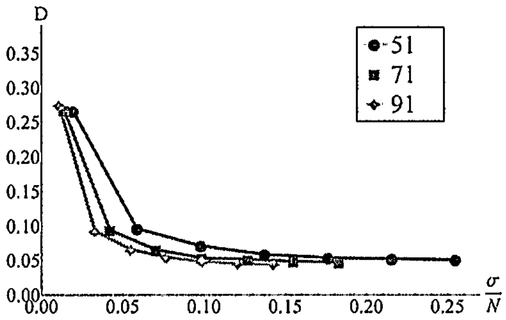 	$\theta\text{out}=\frac{\pi}{4},\ \theta\text{in}=\frac{\pi}{4},\ \Delta\phi=0$ 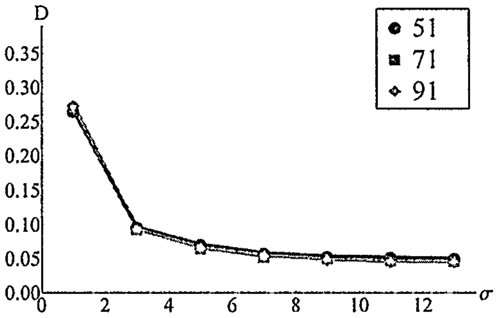
$\theta\text{out}=\frac{\pi}{12},\theta\text{in}=\frac{\pi}{12},\Delta\phi=\frac{\pi}{4}$ 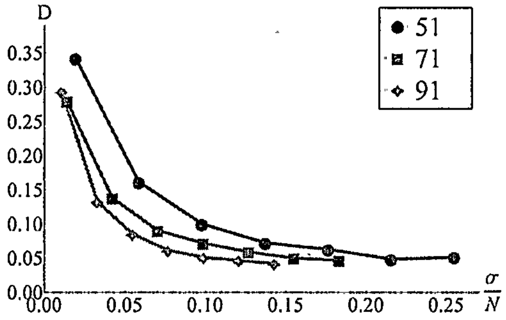 	$\theta\text{out}=\frac{\pi}{12},\ \theta\text{in}=\frac{\pi}{12},\ \Delta\phi=\frac{\pi}{4}$ 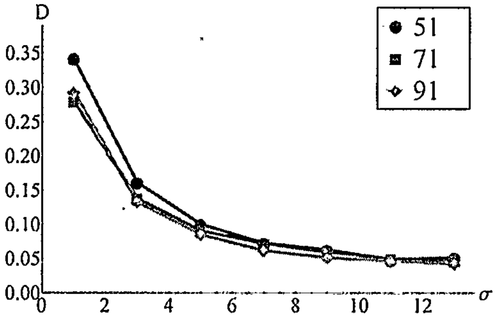 D 0.35 0.30 0.25 0.20 0.15 0.10 0.05 0.00 0 2 4 6 8 10 12 σ ● 51 ▪ 71 ◇ 91